Latin American Journal of Aquatic Research, 53(3): 450-472, 2025
DOI: 10.3856/vol53-issue3-fulltext-3370

Research Article

Phytoplankton community composition in Bahía de Banderas Jalisco-Nayarit, Mexico, during the dry season

Ana Mercedes Cupul-Velázquez[1], Fernando Vega-Villasante[2]
María del Carmen Cortés-Lara[3], Mario Alberto Fuentes-Arreazola[4]
Saúl Rogelio Guerrero-Galván[2] & Amílcar Leví Cupul-Magaña[3]
[1]Post-Graduate Studies in Biosystematics, Ecology and Management of Natural and Agricultural Resources (BEMARENA), Centro Universitario de la Costa University of Guadalajara, Puerto Vallarta, Jalisco, Mexico
[2]Water Quality and Experimental Aquaculture Laboratory, Centro Universitario de la Costa University of Guadalajara, Mexico, Puerto Vallarta, Jalisco, Mexico
[3]Marine Ecology Laboratory, Centro de Investigaciones Costeras, Centro Universitario de la Costa University of Guadalajara, Mexico, Puerto Vallarta, Jalisco, Mexico
[4]Department of Exact Sciences,Centro Universitario de la Costa, University of Guadalajara Puerto Vallarta, Jalisco, Mexico
Corresponding authors: Fernando Vega-Villasante (fvillasante@cuc.udg.mx)
Amilcar Leví Cupul-Magaña (levi.cupul@academicos.udg.mx)

ABSTRACT. The relationship between environmental variables and the phytoplankton community in the dry season in Bahía de Banderas (BB) was analyzed. Sampling was conducted on the north (NC) and south (SC) coasts of the bay in February 2022. Physicochemical variables, nutrients, and pigments of surface and bottom water were measured, and the phytoplankton community structure was studied. The results showed that the highest temperatures were recorded in NC (23.84 ± 8.65°C). The coldest in SC (20.39 ± 2.26°C), salinity (34.06 ± 0.09), and density (24.08 ± 0.82 kg m^{-3}) were highest in SC, while pH, dissolved oxygen, and its saturation and transparency were higher in NC; furthermore, the highest concentrations of nutrients and pigments were recorded in SC, except chlorophyll-*a* which was in NC. A total of 214 phytoplankton species were identified: 88 diatoms, 113 dinoflagellates, 6 silicoflagellates, 2 cyanobacteria, and 1 species for ebriids, haptophytes, euglenophytes, chlorophytes, and ciliates, highlighting the presence of 74 harmful species. Likewise, 83 species were new records for the bay. High cell abundances were recorded in SC (980,440 cells L^{-1}) while in NC was 353,160 cells L^{-1}. The diatoms *Guinardia striata* and *Leptocylindrus danicus* presented high abundances in the bay with 281,360 and 137,460 cells L^{-1}, and the dinoflagellates *Scrippsiella acuminata* and *Karenia mikimotoi* with 80,380 and 55,400 cells L^{-1}, respectively. The environmental variables temperature, salinity, depth, transparency, NH_4^+, NO_2^-, SiO_2^-, and pigments such as chlorophyll-*a* and chlorophyll-*c* recorded in this study explained 96.3% of the correlation with the abundance of the phytoplankton community, evidencing the sensitivity of the community to the hydrographic variability that occurs in the BB during the dry season.

Keywords: marine plankton; environmental variables; microalgae; taxonomic groups, primary productivity; Tropical Pacific off Central Mexico

Associate Editor: José Luis Iriarte

INTRODUCTION

Marine phytoplankton are a group of mostly photosynthetic unicellular microalgae that constitute a crucial component of the marine food web. They contribute approximately 50% of oceanic net primary production and are intimately involved in major biogeochemical cycles in aquatic environments (Round et al. 1990, Field et al. 1998). These cells are sensitive to changes in environmental variables, and their response as bioindicators provides information for understanding the links between phytoplankton, climate, water quality, and anthropogenic activity in aquatic ecosystems (Hays et al. 2005, Hernández-Becerril et al. 2008, Fehling et al. 2012). Quantification of phytoplankton biomass and composition has proven to be an essential tool for understanding the structure and identifying differences between spatial and temporal variables at any scale because communities are highly dynamic and respond rapidly to changes in marine ecosystems (Marshall & Alden 1993, Troccoli-Ghinaglia et al. 2004, Ilyash et al. 2014, Matos et al. 2016, Zheng et al. 2022).

Primary productivity (PP) is limited by nutrient availability and light intensity, where light intensity is higher in oceanic areas and tropical waters. In contrast, it is lower in coastal zones, upwelling areas, and subpolar regions due to the presence of particulate and dissolved material. However, it has been observed that PP is higher in coastal regions, upwelling areas, and subpolar regions during seasonal temperature changes due to higher nutrient levels. Estrada et al. (2016) observed a predominant stratification in the water column of the Atlantic, Indian, and Pacific oceans between 35°N and 40°S, where the surface layers were characterized by low nutrient concentration. The phytoplankton community (PC) consisted mainly of dinoflagellates, while the contribution of diatoms was significant in the coastal zone with shallow nutriclines (e.g. equatorial upwelling regions). In this sense, the results of Chavez (1989) show a clear relationship between cell size and distance offshore, finding that larger phytoplankton aggregates dominate near shore, while small forms <1 µm dominate offshore in the eastern and central tropical Pacific, where surface nutrient concentrations were high in equatorial upwelling coastal areas, with no clear relationship with cell size and nutrient concentration.

In the Tropical Pacific off Central Mexico (TPCM), several studies have been conducted focused on the dominant taxonomic groups (diatoms and dinoflagellates) that constitute a large percentage of the PC in the region, highlighting general descriptions of the composition and distribution of the community in the TPCM (Esqueda-Lara et al. 2005, Hernández-Becerril 2014). Likewise, studies have been carried out evaluating the PP and phytoplankton biomass based on chlorophyll-*a* (Chl-*a*) concentration (*in situ*) and by satellite imagery (López-Sandoval et al. 2009a-b, Cepeda-Morales et al. 2017, Domínguez-Hernández et al. 2020, Pérez-de Silva et al. 2023), as well as under El Niño-La Niña conditions (Pelayo-Martínez et al. 2017, Pérez-de Silva et al. 2023).

Concerning the PC on the coasts of the TPCM (Jalisco, Colima, Michoacán, and Guerrero), Hernández-Becerril et al. (2021) in cruise samples from 2009 to 2019 identified 501 species belonging to 7 taxonomic groups where the most abundant were dinoflagellates (257) and diatoms (195). In this sense, in the southern coast of Jalisco and northern Colima Esqueda-Lara et al. (2005) reported that the best-represented groups were dinoflagellates followed by diatoms, where the 286 species identified 43% of dinoflagellates and 15-25% of diatoms represent the flora described above in the TPCM. At the same time, on the coast of the state of Nayarit, Meave-del Castillo et al. (2001) identified 160 species of planktonic diatoms during summer conditions in 1999, most of which have been reported in the TPCM.

However, in Bahía de Banderas (BB) (western Mexico), few studies have focused on the PC and its ecology has not been sufficiently addressed; this is especially relevant due to the complex hydrographic conditions of the bay, influenced by the presence of tropical cyclones and river discharge in summer, NW winds, upwellings and swells in winter, and the convergence of three ocean current systems in front of the bay (Pantoja et al. 2012, Portela et al. 2016). In general, these mixing conditions are favorable for the development of primary productivity in the region.

In this sense, Cortés-Altamirano et al. (1996-1997) documented for the first time the presence of proliferation in the bay, caused by the ciliate *Mesodinium rubrum*, in April 1995 and January 1996, highlighting that these events are strongly linked to upwelling events, which enriches the euphotic layer. Likewise, Bravo-Sierra (1999) described the planktonic flora in the bay in August 1990, November 1990, and February 1991, totaling 191 species. Diatoms were the most abundant, followed by dinoflagellates.

Since 2000, a long-term monitoring program of the phytoplankton community of BB has recorded a total of 186 species, as well as the identification and quantification of species responsible for harmful algal

blooms (HAB), with 90 events being recorded in the period 2000-2021, where 21 were classified as potentially toxic and 69 harmful, highlighting the year 2011 with nine events, with dinoflagellates being responsible for 70% of these events, diatoms for 20% and raphidophyceae for 10% (Cortés-Lara et al. 2022).

Therefore, the objective of this study was to evaluate the structure and composition of the PC in the dry season using classical diversity descriptors to identify the relationship between environmental variables and the PC present in the BB.

MATERIALS AND METHODS

Study area

Bahía de Banderas (BB) is located in western Mexico, in the TPCM region, conforms between the northern limits of the coast of Jalisco and southern Nayarit between 20°25' and 20°47'N and 105°15' and 105°42'W (Fig. 1). The bay extends approximately 43 km in the N-S (Punta Mita to Cabo Corrientes) direction and 37 km in the E-W direction, defining an area of approximately 1,500 km^2. The region is distinguished by the presence of a submarine canyon more than 1,500 m deep along the south coast of the bay (Plata & Filonov 2007, Kelly-Gutiérrez et al. 2010).

In oceanographic terms, three ocean current systems converge in the TPCM region. In winter and spring, the California Current (CC) flows in an N-S direction from the northeastern Pacific Ocean, providing water with temperatures between 10 and 21°C and salinity <34.6, as well as high concentrations of oxygen and nutrients. The Mexican Coastal Current (MCC), which extends from the Gulf of Tehuantepec to the mouth of the Gulf of California (GC), carries warm water of higher salinity and low nutrients in summer and autumn due to its origin in the eastern equatorial Pacific. The influence of equatorial waves intensifies this current and is more pronounced during El Niño years (Lavín et al. 2006, Zamudio et al. 2007, Pantoja et al. 2012). Finally, the Gulf of California Water mass (GCW) flows southward, permanently contributing water with a temperature >12°C and salinity >35.1. The boundaries between these water masses and the resulting mixing patterns give rise to saline and thermal fronts (Lavín et al. 2009, Portela et al. 2016, Castro et al. 2017). The convergence of the three ocean current systems in front of BB generates a wide variation in water surface temperature throughout the year, reaching maximum values of 30°C in late summer and fall and minimum values of 20°C during winter and spring, with an annual average of 26.4°C (Carriquiry et al. 2001).

Atmospherically, the climate in the region is characterized as warm and sub-humid, classified as Aw1 and Aw2 according to the Köppen classification. The average annual temperature is 26.9°C, with February being the coldest month at 15.4°C and July to October the warmest, with an average of 28°C and an average maximum of 30°C (Morales-Hernández et al. 2013).

The average annual rainfall in the area is 1,000 to 1,500 mm, with a maximum monthly rainfall of 230 mm in June and July (Plata & Filonov 2007). In the bay during the winter and spring, the influence of NW winds generates upwelling events on the southern coast, which causes the sea surface temperature to decrease to 18°C and the thermocline to be located between 20 and 40 m depth (Wyrtki 1965a-b, Griffiths 1968, Fiedler 1992). Likewise, Plata & Filonov (2007) describe how the internal tide influences the bay in the NW part, which gives rise to tidal disintegration processes that form groups of short internal waves. These waves generate instability during their displacement towards the coast, causing mixing in sections of the water column.

Sampling procedure

Physicochemical variables, nutrients, pigments, and phytoplankton were recorded and collected on February 21, 2022, in the dry climatic season at five stations located on the north coast (NC) and five on the south coast (SC) in BB (Fig. 1).

At each station, vertical profiles of temperature (°C), salinity, and density (kg m^{-3}) were obtained using a CTD-SonTek CastAway® from Xylem®. On average, the profiles reached a depth of approximately 20 m in NC and up to 70 m in SC. Complementary pH, dissolved oxygen (mg L^{-1}), and oxygen saturation (%) measurements were taken at the surface (0.3 m), mid-depth, and bottom levels using a YSI-ProDSS probe (Xylem®) with a 20 m depth limit. In the northern transect, some measurements reached the bottom, while in the deeper southern transect, they were limited to the instrument's maximum range. Water transparency (m) was recorded with a Secchi disk of 30 cm diameter.

At all stations, water samples were collected from both the surface (0.30 m) layer and the bottom (NC 7-25 m; SC 25 m) using a 1.7 L Niskin water sampler bottle (General Oceanics®). To analyze nutrient concentration, 1 L of the sample was stored in Nalgene bottles®, after which 100 µL of $HgCl_2$ (Kirkwood 1992) was added. For pigments, 1 L of sample was stored in Nalgene® bottles and kept at 4°C for subsequent laboratory analysis. For the identification and quantifi-

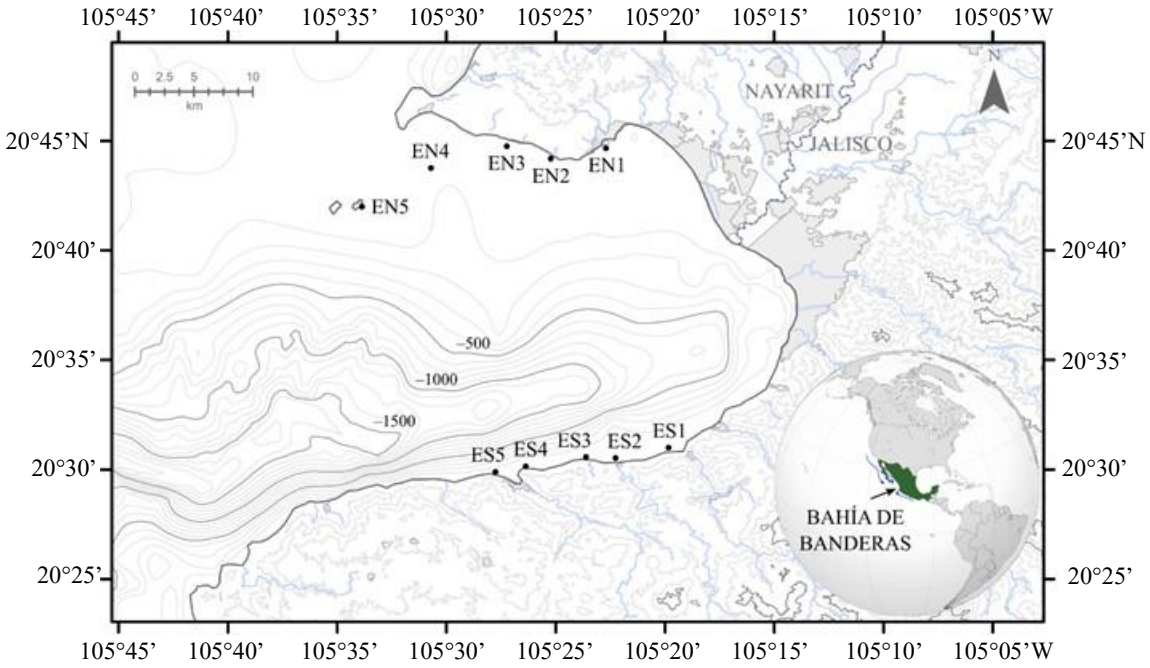

Figure 1. Location of Bahía de Banderas, Jalisco-Nayarit, Mexico, in the Tropical Pacific off Central Mexico (TPCM) and location of sampling stations (EN: north coast, ES: south coast). Isobaths at every 100 m (GEBCO 2022). Main surface runoff and contour lines every 200 m (INEGI 2022a-b). Datum: WGS-84.

cation of the PC, 500 mL polyethylene bottles were used and preserved with a 1:100 Lugol solution.

Laboratory procedure

Nutrients

The water samples were filtered through a cellulose membrane Millipore® filter 0.45 µm pore size with a diameter of 47 mm and were kept refrigerated (4°C). To determine the concentration of nutrients by colorimetry, the phenol-hypochlorite method (Solórzano 1969) was used for ammonium (NH_4^+), sulfanilamide and NED method for nitrite (NO_2^-), nitrate (NO_3^-) Cd-Cu reduction method, phosphate (PO_4^{3-}) ascorbic acid method and silicate (SiO_2) metol-sulfite method (Strickland & Parsons 1972).

Pigments

The samples were filtered through GF/F Whatman® glass fiber filters of 47 mm diameter and 0.7 µm pore size. The filters were then deposited in amber glass vials containing 10 mL of 100% methanol, using the Holm-Hansen & Riemann (1978) modification, and subsequently stored at -20°C for 24 h. The extraction and calculation of pigment concentration was performed following the technique and equations of Strickland & Parsons (1972). For nutrients and pigments, the absorbances were measured in a Thermo Scientific™ Orion™ AquaMate 7000 Vis spectrophotometer.

Phytoplankton

Water samples for the identification and quantification of the PC were concentrated in triplicate using a sedimentation chamber with 50 mL columns and left to stand in the dark for a period of 24 h according to the Utermöhl method described in Reguera et al. (2011). Subsequently, phytoplankton organisms were identified at the species level with a Leica DME microscope at 10x magnification by checking the entire bottom of the chamber. The identification of the different phytoplankton species was performed using taxonomic systematics with identification keys for the TPCM and GC: Licea et al. (1995), Moreno et al. (1996), Gárate-Lizárraga et al. (2009), Esqueda-Lara & Hernández-Becerril (2010), Gárate-Lizárraga (2012, 2014a-b), Hernández-Becerril et al. (2021), among other authors.

Statistical analysis

Descriptive statistics (mean, standard deviation, and interval) were estimated for hydrographic features, nutrients, pigments, and phytoplankton. Subsequently, the statistical assumptions of normality and homoscedasticity were evaluated with the Kolmogorov-Smirnov test. To determine the existence of significant

differences between collection sites in BB, a non-parametric test, the Kruskal-Wallis (H) and Dunn's (Q) *a posteriori* tests, were applied, with a significance level of $P < 0.05$. The statistical analysis was performed using SigmaPlot v11 software.

With the abundance of the species that make up the PC by station and depth, the assemblage descriptors: species richness (S), Shannon's diversity (H', bits), Pielou's evenness (J'), Simpson's dominance (λ) and codominance (1-λ) were estimated using PRIMER v6.1.6 software. Additionally, to rank the species according to their abundance and presence in the bay, Olmstead-Tukey (OT) diagrams were constructed (Sokal & Rohlf 1981).

Finally, to evaluate the relationship between environmental variables and the PC, a canonical correspondence analysis (CCA) was performed using the Canoco software package for Windows v4.5 with a Monte Carlo permutation test (ter Braak 1986). These data were pretreated previously with the fourth root ($\sqrt[4]{}$)to reduce the contribution of the most abundant species and increase the contribution of those with very low abundance. In addition, multicollinearity among environmental variables was assessed using the variance inflation factor (VIF < 10) method, which is lower than ten to avoid severe multicollinearity (Chatterjee & Hadi 2012) and to influence the results of the CCA. The biplots were generated using CanoDraw for Windows (ter Braak & Smilauer 2002). The hydrographic features, nutrients, and pigment sections were generated using Ocean Data View v5.7 software (Schlitzer 2024). The vertical resolution of the discrete samples was limited to 25 m, except for temperature, salinity, and density, which were obtained from CTD data.

RESULTS

Hydrographic features, nutrients, and pigments

The average values of the physicochemical parameters recorded during the monitoring campaign are presented (Table 1). The NC presented higher values of temperature, pH, dissolved oxygen, oxygen saturation, and transparency compared to the SC. While in the SC, higher values of salinity and density were recorded.

Figure 2 show the horizontal and vertical distribution of the physicochemical variables on both coasts. The NC, characterized by a shallower depth, presented a higher temperature gradient (ΔT_{CN} = -0.162 ± 0.050°C m^{-1}) compared to the deeper SC (ΔT_{CS} = -0.062 ± 0.008°C m^{-1}). Also, NC presented higher gradients of salinity ($\Delta S_{CN} = 0.004 \pm 0.007$) and density ($\Delta \rho_{CN}$ = 0.049 ± 0.017 (kg m^{-3}) m^{-1}) but lower mean salinity in the bottom and density in the surface concerning SC ($\Delta S_{CS} = 0.002 \pm 0.001$ and $\Delta \rho_{CS} = 0.022$ ± 0.002 (kg m^{-3}) m^{-1}) with higher mean values in the bottom (Fig. 2), respectively. Likewise, the northern transect exhibited a relatively weakly stratified water column, with an average stratification value (φ) of 92.82 J m^{-3}, in contrast to the southern transect, which showed strong stratification with a φ value of 1093.82 J m^{-3}, calculated as Simpson (1981).

In the NC, subtle increases in gradients were observed, possibly associated with the thermocline, halocline, and pycnocline around 20 m depth, towards the end of the profile at more oceanic stations. These features may also be influenced by wind-driven mixing, tidal forcing, mesoscale activity, and internal waves. Particularly during the northern transect, strong winds were experienced, resulting in slight swells. In contrast, in the SC, these gradients were identified at approximately 50 m depth, likely due to calm sea surface and wind conditions.

Despite these differences in stratification, values of pH, dissolved oxygen, and oxygen saturation for both coasts were similar (Fig. 2). It is plausible, particularly within the upper 20 m, where biological activity and atmospheric exchange may exert a more uniform influence. Additionally, the comparable sampling depths (limited to 20 m) may not capture the full extent of stratification at the deeper site, potentially leading to similar near-surface biogeochemical conditions.

In this sense, the Kruskal-Wallis test revealed significant differences in environmental variables (temperature, salinity, density, station depth, and transparency, $P < 0.05$) across the analyzed stations (Table 1). However, the variables pH, dissolved oxygen, and oxygen saturation did not show any significant differences ($P > 0.05$).

Table 2 summarizes the average values and interval of variation of nutrients determined for BB during the monitoring campaign. The maximum values of NH_4^+ and NO_2^- were recorded for NC, whereas, in SC, the highest values of NO_3^-, PO_4^{3-}, and SiO_2 were estimated. Figure 3 show the vertical and horizontal variation of NH_4^+ for both coasts of the bay, where high and the lowest average concentrations (4.10 and 3.92 µM) were recorded in the bottom and the surface of the NC. On the other hand, the SC presents an integrated average value of 4.05 µM for the section, except for the last station, which presented minimal availability of this micronutrient. The NO_2^- concentration distribution on both coasts (Fig. 3) shows higher values at the bottom of the sections, suggesting a possible upward trend of

Table 1. Summary of mean, standard deviation (SD), interval, and station recordings of physicochemical variables for sampling stations along the coast of Bahía de Banderas, Jalisco-Nayarit, Mexico, in February 2022. 1: CTD data, 2: YSI-ProDSS. In bold: significant differences.

Physicochemical	Mean ± SD	Station	Min	Max	Station	*H*	*P*
Temperature (°C)[1]	21.03 ± 1.90	ES5	17.73	25.91	EN1	512.23	**0.001**
Salinity (S_p)[1]	34.01 ± 0.07	EN4	33.70	34.19	ES5	264.60	**0.001**
Density (kg m^{-3})[1]	23.85 ± 0.65	EN1	22.31	25.03	ES5	431.26	**0.001**
pH[2]	8.22 ± 0.15	ES1	7.99	8.47	EN2	10.16	0.34
Dissolved oxygen (mg L^{-1})[2]	5.75 ± 2.10	EN5	2.58	8.90	EN1	7.89	0.55
Oxygen saturation (%)[2]	82.53 ± 32.10	EN5	35.70	133.10	EN1	7.91	0.54
Station depth (m)[1]	42.26 ± 29	EN1	7.54	74.94	EN2	19.00	**0.03**
Transparency (m)	4.73 ± 0.67	ES5	3.05	5.20	ES1	19.00	**0.03**

this chemical compound, which is consumed very quickly at the surface, showing the lowest values with an evident pattern in the surface stations of the NC. In this sense, the minimum availability of NO_3^- was determined in the shallow portion of the NC, and an increase of this element at depth was observed for both coasts of the bay (Fig. 3). Similar patterns were determined for PO_4^{3-} and SiO_2 (Fig. 3), respectively. Nevertheless, the Kruskal-Wallis test revealed no significant differences in nutrients ($P > 0.05$) across the analyzed stations (Table 2).

The mean values and intervals of variation of pigments calculated for both coasts of BB are given in Table 3. The highest means concentrations of chlorophyll-*a* (Chl-*a*), chlorophyll-*b* (Chl-*b*), chlorophyll-*c* (Chl-*c*), chlorophytes-cyanophytes carotenoids (Chlo-Cya CARs), chrysophytes-pyrrhophytes carotenoids (Chr-Py CARs) were recorded at the surface on the SC and phaeopigments (Pheo) were estimated in the bottom for the SC, the lowest mean concentrations were determined for the surface of the NC (Fig. 4). In contrast, it is observed that two stations present a high concentration of pigments, except for Pheo, as an algal bloom could be detected in EN2 at the bottom and ES5 on the surface. The Kruskal-Wallis test revealed no significant differences in pigments ($P > 0.05$) across the analyzed stations on the bay (Table 3).

Phytoplankton composition and structure

A total of 214 species were identified, classified into nine groups: dinoflagellates (113 species, 52.80%), diatoms (88 species, 41.12%), silicoflagellates (6 species, 2.80%), cyanobacteria (2 species, 0.93%), ebridians (1 species, 0.47%), haptophytes (1 species, 0.47%), euglenophytes (1 species, 0.47%), chlorophytes (1, 0.47%) and ciliates (1 species, 0.47%). It was highlighted that for this study, 83 new records were identified for the BB, grouped into 61 dinoflagellates, 16 diatoms, 2 silicoflagellates, 1 cyanobacterium, 1 ebridian, 1 haptophyte, and 1 chlorophyte. We also identified 74 species classified as forming algal blooms, 40 dinoflagellates, 25 diatoms, 4 silicoflagellates, 2 cyanobacteria, and 1 species for haptophytes, euglenophytes and ciliates (Table 4).

In terms of total cell abundance (1,333,600 cells L^{-1}), diatoms were the most abundant group (819,420 cells L^{-1}, ~61%), followed by the group consisting of dinoflagellates (403,520 cells L^{-1}, ~30%); in contrast, the group with the lowest presence was chlorophytes (60 cells L^{-1} <0.005%). The average cell abundance for each group is shown in Table 5. In this sense, it was determined that the diatoms group had the highest presence in the SC, while the dinoflagellates group in the NC (Fig. 5). Diatom species: *Guinardia striata* (281,360 cells L^{-1}, ~21%), *Leptocylindrus danicus* (137,460 cells L^{-1}, ~10%), *Chaetoceros compressus* (60,820 cells L^{-1}, ~4.5%) and of dinoflagellates: *Scrippsiella acuminata* (80,380 cells L^{-1}, ~6%), *Karenia mikimotoi* (55,400 cells L^{-1}, ~4.1%), *Alexandrium tamiyavanichii* (38,900 cells L^{-1}, ~3%), were the most abundant concerning total cell abundance in the bay.

Overall, cell richness and abundance were higher in the SC, with maximum values of 180 species and 980,440 cells L^{-1}, respectively, while in the NC, there were 159 species and 353,160 cells L^{-1}. However, the Shannon's diversity index for both coasts was high (H' 4.90 bits). The average Pielou's evenness index (J' = 0.61 ± 0.08) suggests that the community presents a mixed distribution, where there is a certain dominance of some species. Still, there is a high contribution of less common species, which prevails the advantage of some species with a slightly dominant role ($\lambda = 0.17 \pm 0.07$), with high codominance ($1-\lambda = 0.83 \pm 0.07$). Concerning

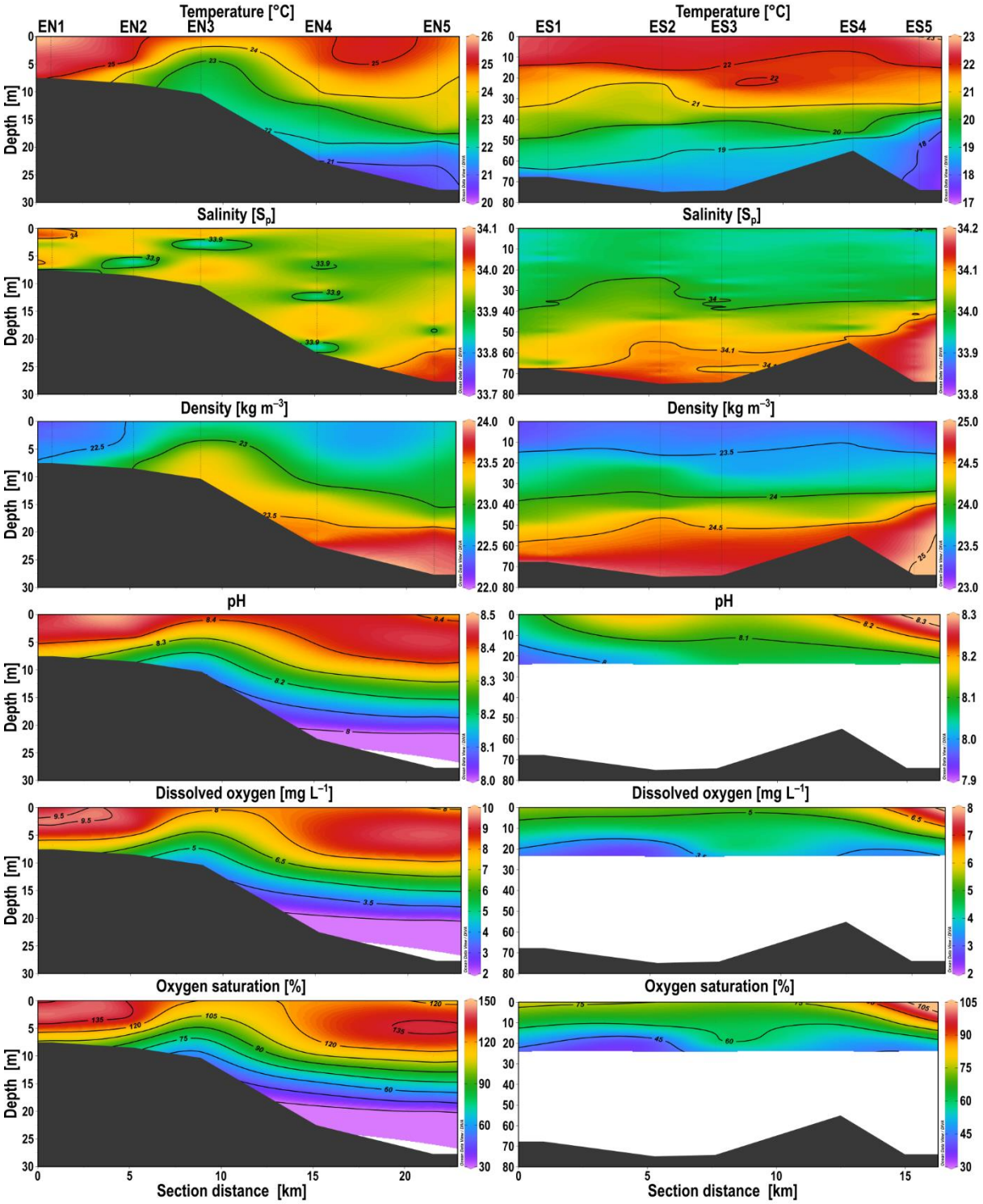

Figure 2. Horizontal and vertical distribution of physicochemical variables for the north (left panel) and south (right panel) coasts of Bahía de Banderas, Jalisco-Nayarit, Mexico in February 2022. Sampling stations; EN: north coast, ES: south coast.

species density and their descriptor indices, no significant differences were determined among the analyzed stations ($P > 0.05$) (Table 6).

Based on the frequency of occurrence and relative species abundance, an Olmstead-Tukey classification diagram was constructed, where 78 species were classified as dominant, corresponding to 39 dinoflag-

Table 2. Summary of mean, standard deviation (SD), interval, and station recordings of nutrient variables for sampling stations along the coast of Bahía de Banderas, Jalisco-Nayarit, Mexico in February 2022.

Nutrients (µM)	Mean ± SD	Station	Min	Max	Station	*H*	*P*
Ammonium (NH_4^+)	4.03 ± 0.55	EN4	3.03	4.95	EN2	8.03	0.53
Nitrite (NO_2^-)	0.34 ± 0.27	EN1,4,5	0.02	0.99	EN4	6.03	0.74
Nitrate (NO_3^-)	3.53 ± 3.09	NC	0.00	8.27	ES2	10.29	0.33
Phosphate (PO_4^{3-})	0.93 ± 0.46	EN1	0.31	1.56	ES2	10.42	0.32
Silicate (SiO_2)	6.51 ± 2.89	EN1	0.71	11.85	ES2	10.71	0.30

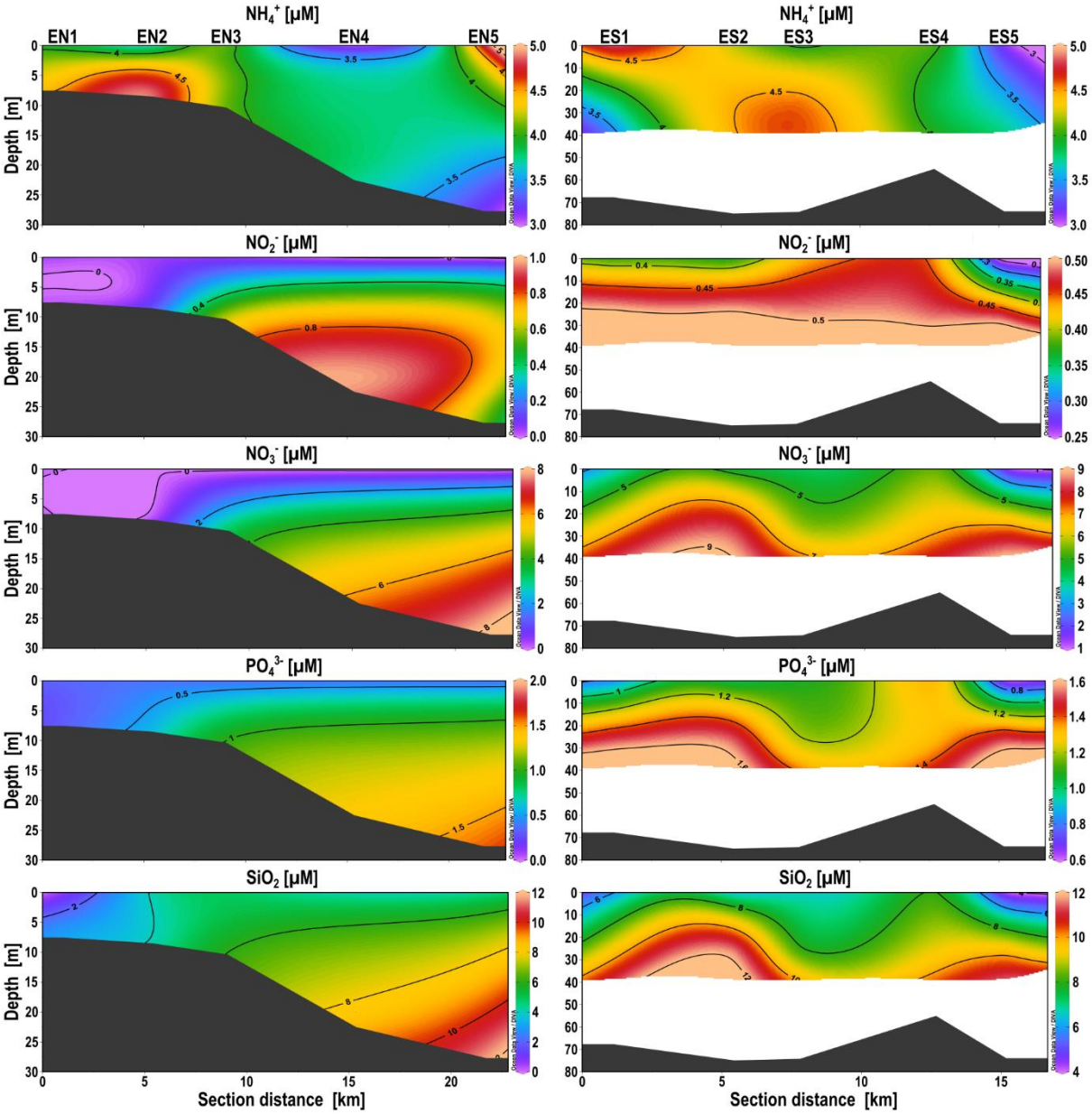

Figure 3. Horizontal and vertical distribution of nutrients for the north coast (left panel) and south coast (right panel) of Bahía de Banderas, Jalisco-Nayarit, Mexico in February 2022. Sampling stations; EN: north coast, ES: south coast.

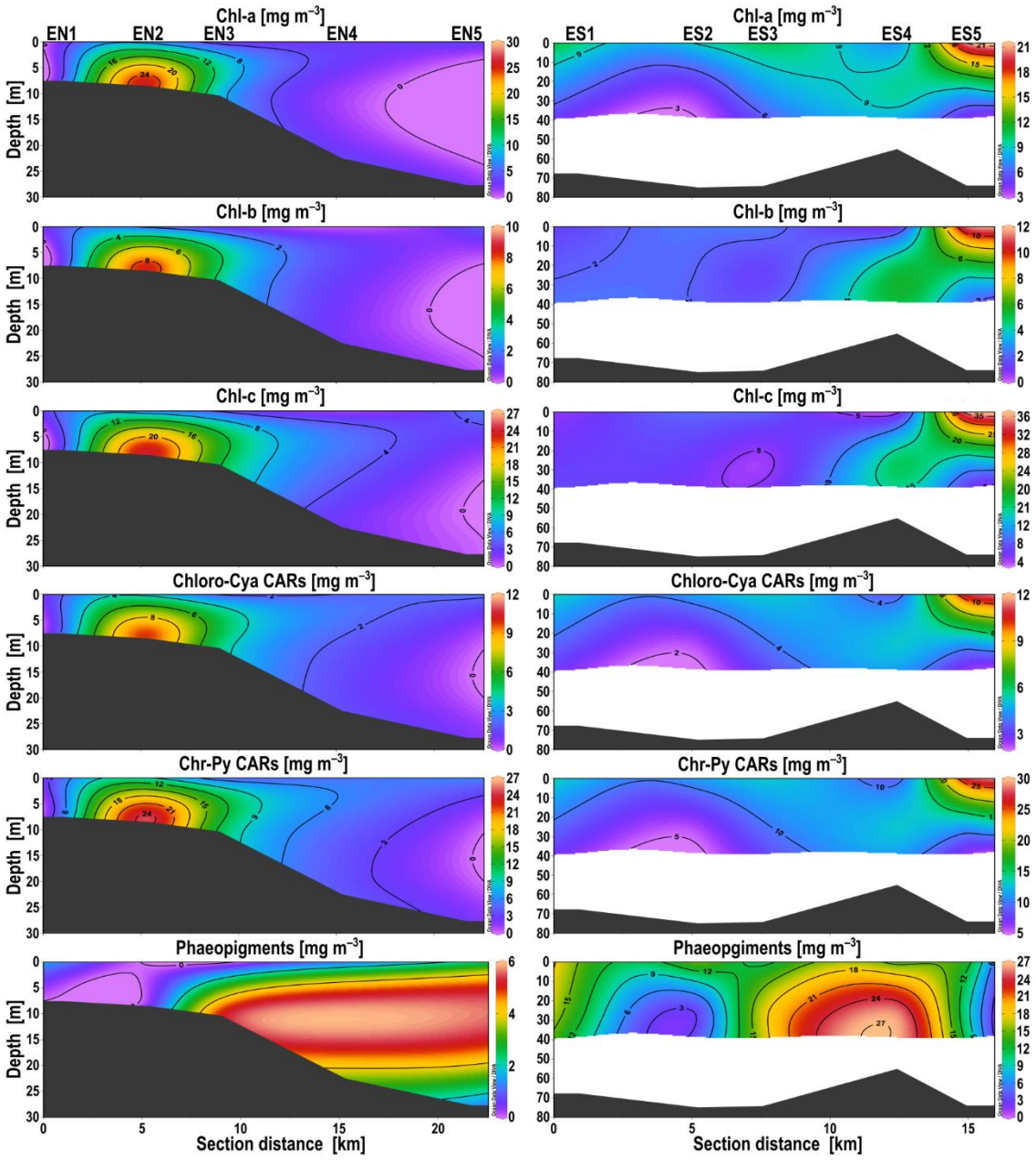

Figure 4. Horizontal and vertical distribution of pigments for the north coast (left panel) and the south coast (right panel) of Bahía de Banderas, Jalisco-Nayarit, Mexico, in February 2022. Sampling stations; EN: north coast, ES: south coast.

ellates, 34 diatoms, 4 silicoflagellates and 1 ciliate. This group represented 89.41% of the total relative abundance. The group of constant species consisted of 10 species: 7 dinoflagellates, 2 diatoms, and 1 euglena, representing 0.25% of the total. The group of occasional species consisted of 28 species: 15 diatoms, 8 dinoflagellates, 2 silicoflagellates, 2 cyanobacteria, and 1 haptophyte, representing 9.48% of the total abundance. The species classified as rare comprised 98, corresponding to 59 dinoflagellates, 37 diatoms, 1 ebridian, and 1 chlorophyte, accounting for 0.86% of the total abundance (Fig. 6, Table 4).

Within the group of dominant species, a second classification was made based on relative abundance (>0.5%) reducing from 78 to 30 dominant species consisting of the diatoms *Cerataulina pelagica*, *Chaetoceros* spp., *C. compressus*, *C. didymus*, *C. socialis*, *Coscinodiscus* spp., *Dactyliosolen mediterraneus*,

Table 3. Summary of mean, standard deviation (SD), interval, and station recordings of pigments variables for sampling stations along the coast of Bahía de Banderas, Jalisco-Nayarit, Mexico, in February 2022.

Pigments (mg m^{-3})	Mean ± SD	Station	Min	Max	Station	*H*	*P*
Chlorophyll-*a*	7.84 ± 6.57	EN5	1.34	28.11	EN2	14.29	0.11
Chlorophyll-*b*	2.69 ± 2.98	EN5	0.18	11.52	ES5	12.14	0.21
Chlorophyll-*c*	8.77 ± 8.94	EN5	0.44	36.72	ES5	12.31	0.20
Chlorophytes-cyanophytes-carotenoids	3.99 ± 2.73	EN5	0.76	11.12	ES5	13.45	0.14
Chrysophytes-pyrrhophytes- carotenoids	9.98 ± 6.82	EN5	1.90	27.80	ES5	13.45	0.14
Phaeopigments	7.70 ± 7.64	EN1,2,3	0.00	26.38	ES4	15.02	0.09

Detonula pumila, *Guinardia flaccida*, *G. striata*, *Haslea gretharum*, *Leptocylindrus danicus*, *Lioloma pacificum*, *Proboscia alata*, *Thalassionema frauenfeldii*, *Thalassiosira aestivalis*, and *Thalassiosira* spp.; the dinoflagellates *Alexandrium tamiyavanichii*, *Karenia mikimotoi*, *Margalefidinium polykrikoides*, *Polykrikos hartmannii*, *Preperidinium meunieri*, *Prorocentrum gracile*, *P. lima*, *P. micans*, *Protoperidinium* spp., *P. pellucidum*, *Scrippsiella acuminata*, and *Tripos furca* and the ciliate: *Mesodinium rubrum*, with which the CCA analysis was carried out.

It is observed that the variability of the sampling sites in the SC is more related to nutrients, salinity (Sal), and depth (Pf). In contrast, the NC sites are more related to temperature (Tem) and water transparency (Tran) (Fig. 7). Figure 7 shows that the central diatoms species (12) and pennates (2) are more related to the characteristics present in SC. At the same time, dinoflagellates and ciliates are more related to the characteristics of the NC. According to the CCA, the two main axes showed a cumulative correlation of 96.3% between species and environmental variables, explaining 73.9% (axis1 = 61.9% and axis2 = 12%) of the variance between the relationship of environmental variables and dominant species of the PC of BB in February 2022 (Fig. 7, Table 7). The variables Tem, Pf, Sal, NO_2^- and SiO_2 were associated on axis 1. The dominant phytoplankton species linked to this axis were diatoms: *Cerataulina pelagica*, *Chaetoceros* spp., *C. compressus*, *C. didymus*, *C. socialis*, *Dactyliosolen mediterraneus*, *Detonula pumila*, *Guinardia flaccida*, *G. striata*, *Leptocylindrus danicus*, *Lioloma pacificum*, *Proboscia alata*, *Thalassionema frauenfeldii*, *Thalassiosira aestivalis*, the dinoflagellates *Alexandrium tamiyavanichii*, *Polykrikos hartmannii*, *Preperidinium meuneri*, *Prorocentrum gracile*, *P. lima*, *Protoperidinium* spp., *P. pellucidum*, *Scrippsiella acuminata* and the ciliate *Mesodinium rubrum* (Table 4, Fig. 7). On the other hand, the transparency variables (Tran), NH_4^+, Chl-*a* and Chl-*c*, as well as the dominant diatom species *Coscinodiscus* spp., *Haslea gretharum*, *Thalassiosira* spp; the dinoflagellates *Karenia mikimotoi*, *Margalefidinium polykrikoides*, *Prorocentrum micans* and *Tripos furca* (Table 4, Fig. 7) were associated with axis 2. The variables that showed the greatest influence on the community during this season were temperature (Tem), salinity (Sal), transparency (Tran), depth (Pf), NH_4^+, SiO_2 and NO_2^- and the pigments Chl-*α* and Chl-*c*. However, the interactions between the canonical axes were not significant according to the Monte Carlo test with 9,999 permutations ($P = 0.1099$).

DISCUSSION

Hydrographic features, nutrients, and pigments

The lowest sea surface temperatures are recorded in BB during the winter and spring (dry season). It is the result of a set of processes involving the thermal equilibrium between the water surface and the relatively low-temperature atmosphere, the influence of NW winds associated with the intensification of the CC, swells, and coastal upwelling events (vertical advection) in the SC of the bay, which subsequently moves this mass of bottom water in the direction of the NC. These mechanisms carry out the fertilization of the waters, favoring the increase of primary productivity in the bay. The hydrographic characteristics observed in this study are typical of the dry period in the TPCM region, where BB is located (López-Sandoval et al. 2009a-b, Cepeda-Morales et al. 2017, Cortés-Lara et al. 2022, Pérez-de Silva et al. 2023).

This condition can be seen in the temperature distribution on the NC and SC in the BB, where the lowest temperature values were found in the SC, while in the NC these are higher; however, in this last section the intrusion of colder water can be seen from the deepest stations to the shallowest ones (Fig. 2), which may be a consequence of the upwelling event that occurred in the days before sampling (February 18) (NOAA 2024). The temperature distribution in NC exhibits weak stratification (92.82 J m^{-3}), with a thick-

Table 4. Phytoplankton species composition in coasts of Bahía de Banderas (BB), Jalisco-Nayarit, Mexico in February 2022. OT: Olmstead-Tukey test classification: R: rare, C: constant, O: occasional, D: dominant. Species location: north coast (NC), south coast (SC). In addition, new records to BB are indicated as (*), and Harmful algal bloom species as (+).

ID	Species	OT	NC	SC	ID	Species	OT	NC	SC
	Diatoms					**Diatoms (cont.)**			
1	*Actinocyclus cuneiformis*	R	X	X	50	*Guinardia striata*$^{+}$	D	X	X
2	*Amphora* spp.	R	X	X	51	*Haslea gretharum*$^{+}$	D	X	X
3	*Asterionella formosa**	R		X	52	*Haslea wawrikae*$^{+}$	R	X	X
4	*Asteromphalus elegans**	R		X	53	*Helicotheca tamesis*	D	X	X
5	*Asteromphalus flabellatus*	C	X	X	54	*Hobaniella longicruris*	R	X	X
6	*Asteromphalus heptactis*$^{+}$	R		X	55	*Leptocylindrus danicus*$^{+}$	D	X	X
7	*Bacteriastrum hyalinum*	O		X	56	*Licmophora abbreviata*	R	X	X
8	*Biddulphia alternans*	D	X	X	57	*Lioloma pacificum*	D	X	X
9	*Biddulphia biddulphiana*	R	X	X	58	*Mastogloia* spp.	R		X
10	*Biddulphiella tridens**	D	X	X	59	*Meuniera membranacea**	R	X	
11	*Caloneis westii**	C	X	X	60	*Navicula* spp.	D	X	X
12	*Cerataulina pelagica*$^{+}$	D		X	61	*Neocalyptrella robusta*	D	X	
13	*Chaetoceros affinis*	D		X	62	*Nitzschia linearis**	R	X	
14	*Chaetoceros coarctatus*$^{+}$	O	X	X	63	*Nitzschia* spp.	D	X	X
15	*Chaetoceros compressus*	D	X	X	64	*Odontella aurita*	R	X	X
16	*Chaetoceros curvisetus*$^{+}$	O		X	65	*Palmerina hardmaniana**	R	X	
17	*Chaetoceros danicus*$^{+}$	R		X	66	*Paralia sulcata*$^{+}$	R		X
18	*Chaetoceros diadema**	O		X	67	*Planktoniella muriformis**	R	X	
19	*Chaetoceros didymus*	D		X	68	*Planktoniella sol*	D	X	X
20	*Chaetoceros lorenzianus*$^{+}$	R	X		69	*Pleurosigma* spp.$^{+}$	D	X	X
21	*Chaetoceros messanensis*	R		X	70	*Proboscia alata*$^{+}$	D	X	X
22	*Chaetoceros peruvianus*$^{+}$	R		X	71	*Proboscia indica*	D	X	X
23	*Chaetoceros socialis**$^{+}$	D	X	X	72	*Pseudo-nitzschia pungens*$^{+}$	O	X	
24	*Chaetoceros* spp.$^{+}$	D	X	X	73	*Pseudo-nitzschia* spp.$^{+}$	O	X	
25	*Climacodium frauenfeldianum*	O	X	X	74	*Rhizosolenia clevei*	R		X
26	*Corethron hystrix**	O		X	75	*Rhizosolenia hyalina*	R	X	X
27	*Coscinodiscus asteromphalus*	R		X	76	*Rhizosolenia imbricata*$^{+}$	R	X	X
28	*Coscinodiscus centralis*$^{+}$	D	X	X	77	*Skeletonema costatum*$^{+}$	O	X	X
29	*Coscinodiscus gigas*	D	X	X	78	*Stephanocyclus meneghinianus*	R	X	X
30	*Coscinodiscus granii*	R	X	X	79	*Striatella unipunctata*	R	X	
31	*Coscinodiscus perforatus**	O	X	X	80	Thalassionema frauenfeldii	D	X	X
32	*Coscinodiscus radiatus*	R		X	81	*Thalassionema nitzschioides*$^{+}$	D	X	X
33	*Coscinodiscus wailesii*$^{+}$	R	X	X	82	*Thalassiosira aestivalis*$^{+}$	D	X	X
34	*Coscinodiscus* spp.	D	X	X	83	*Thalassiosira gravida*$^{+}$	O	X	X
35	*Dactyliosolen mediterraneus**	D	X	X	84	*Thalassiosira punctigera**	O	X	X
36	*Detonula pumila*	D	X	X	85	*Thalassiosira* spp.	D	X	X
37	*Diploneis crabro**	R	X		86	*Triceratium favus*	R		X
38	*Diploneis stroemii**	R	X		87	*Trieres mobiliensis*	R	X	X
39	*Ditylum brightwellii*$^{+}$	D	X	X	88	*Trieres sinensis**	D		X
40	*Entomoneis alata**	R	X			**Dinoflagellates**			
41	*Eucampia cornuta*	R		X	89	*Actiniscus pentasterias**	R	X	X
42	*Eucampia zodiacus*	O		X	90	*Akashiwo sanguinea*$^{+}$	R	X	
43	*Eupyxidicula palmeriana*	R		X	91	*Alexandrium tamiyavanichii**$^{+}$	D	X	X
44	*Eupyxidicula turris*	D	X	X	92	*Amphidinium carterae**$^{+}$	O	X	X
45	*Fragilariopsis doliolus*	D	X	X	93	*Amphisolenia bidentata*	C	X	X
46	*Gossleriella tropica*	O	X		94	*Asterodinium gracile**	R		X
47	*Grammatophora marina*	R	X	X	95	*Blepharocysta splendor-maris*	D	X	X
48	*Grammatophora oceanica**	O	X		96	*Blixaea quinquecornis*$^{+}$	O	X	X
49	*Guinardia flaccida*$^{+}$	D	X	X	97	*Ceratocorys horrida*	R	X	

Continuation

ID	Species	OT	NC	SC	ID	Species	OT	NC	SC
	Dinoflagellates (cont.)					**Dinoflagellates (cont.)**			
98	*Corythodinium biconicum**	R	X		149	*Protoperidinium abei**	R		X
99	*Corythodinium diploconus**	R		X	150	*Protoperidinium bipes*	R		X
100	*Corythodinium tesselatum**	R	X	X	151	*Protoperidinium bispinum**	R		X
101	*Cucumeridinium coeruleum**	R	X	X	152	*Protoperidinium claudicans**	D	X	X
102	*Dinophysis acuminata*$^{+}$	R	X		153	*Protoperidinium compressum**	D	X	
103	*Dinophysis amandula**	R	X		154	*Protoperidinium conicum*	D	X	X
104	*Dinophysis caudata*$^{+}$	D	X	X	155	*Protoperidinium crassipes**$^{+}$	O	X	X
105	*Dinophysis fortii*$^{+}$	D	X	X	156	*Protoperidinium curvipes**	R	X	
106	*Dinophysis parvula**	R		X	157	*Protoperidinium depressum*	R	X	
107	*Diplopsalis lenticula**	D	X	X	158	*Protoperidinium divergens*$^{+}$	D	X	X
108	*Gonyaulax digitalis*$^{+}$	R	X		159	*Protoperidinium elegans*	D	X	X
109	*Gonyaulax fusiformis**	R		X	160	*Protoperidinium excentricum**	C	X	X
110	*Gonyaulax polygramma*$^{+}$	D	X	X	161	*Protoperidinium grande**	R	X	
111	*Gonyaulax spinifera*$^{+}$	D	X	X	162	*Protoperidinium latispinum*	C	X	
112	*Gonyaulax turbynei*$^{+}$	R	X		163	*Protoperidinium leonis**	D	X	X
113	*Gymnodinium catenatum*$^{+}$	O		X	164	*Protoperidinium obtusum**	R		X
114	*Gymnodinium fuscum**	R	X		165	*Protoperidinium oceanicum*	R	X	X
115	*Gymnodinium impudicum**$^{+}$	O	X		166	*Protoperidinium oviforme**	C	X	X
116	*Gymnodinium simplex**	D	X	X	167	*Protoperidinium ovum**	R	X	X
117	*Gyrodinium dominans**	R	X	X	168	*Protoperidinium pacificum**	R	X	X
118	*Gyrodinium spirale**	D	X	X	169	*Protoperidinium pellucidum*	D	X	X
119	*Heterocapsa* sp.*	R		X	170	*Protoperidinium pentagonum**	O		X
120	*Heterodinium murrayi**	R		X	171	*Protoperidinium punctulatum**	R	X	
121	*Histioneis cymbalaria**	R	X		172	*Protoperidinium pyriforme**	R	X	
122	*Karenia mikimotoi**$^{+}$	D	X	X	173	*Protoperidinium* spp.	D	X	X
123	*Karenia papilionacea**$^{+}$	R		X	174	*Pseliodinium fusus**	D	X	X
124	*Lingulodinium polyedra*$^{+}$	D	X	X	175	*Ptychodiscus noctiluca**	R	X	
125	*Margalefidinium polykrikoides*$^{+}$	D	X	X	176	*Pyrocystis fusiformis*	R	X	X
126	*Noctiluca scintillans*$^{+}$	R		X	177	*Pyrocystis lunula*	C	X	X
127	*Ornithocercus assimilis**	R	X	X	178	*Pyrocystis pseudonoctiluca*	D	X	X
128	*Ornithocercus splendidus**	R		X	179	*Pyrophacus horologium*	R	X	
129	*Ornithocercus thumii*	R		X	180	*Pyrophacus steinii*$^{+}$	C	X	X
130	*Ostreopsis siamensis**$^{+}$	R	X	X	181	*Scrippsiella acuminata*$^{+}$	D	X	X
131	*Oxytoxum globosum**	R		X	182	*Scrippsiella spinifera**$^{+}$	D	X	X
132	*Oxytoxum lingusticum**	R		X	183	*Torquentidium convolutum**$^{+}$	R		X
133	*Oxytoxum scolopax**	R		X	184	*Triadinium polyedricum**	R	X	X
134	*Oxytoxum sphaeroideum**	R	X		185	*Tripos arcuatus**	R	X	
135	*Pentapharsodinium dalei*$^{+}$	D	X	X	186	*Tripos azoricus**	R	X	X
136	*Phalacroma doryphorum**	C	X	X	187	*Tripos brevis*	D	X	X
137	*Phalacroma oxytoxoides**$^{+}$	O	X	X	188	*Tripos candelabrum*	R	X	X
138	*Podolampas palmipes*	R	X	X	189	*Tripos extensus*	R		X
139	*Polykrikos hartmannii**$^{+}$	D	X	X	190	*Tripos furca*$^{+}$	D	X	X
140	*Polykrikos kofoidii*$^{+}$	O	X	X	191	*Tripos fusus*$^{+}$	D	X	X
141	*Preperidinium meunieri*	D	X	X	192	*Tripos gallicus*	R	X	X
142	*Prorocentrum compressum*$^{+}$	D	X		193	*Tripos gravidus*	R		X
143	*Prorocentrum cordatum*$^{+}$	D	X	X	194	*Tripos hircus**$^{+}$	R	X	
144	*Prorocentrum gracile*$^{+}$	D	X	X	195	*Tripos lineatus*$^{+}$	R		X
145	*Prorocentrum lima**$^{+}$	D	X	X	196	*Tripos longirostrum**	R	X	
146	*Prorocentrum micans*$^{+}$	D	X	X	197	*Tripos macroceros*	D	X	X
147	*Prorocentrum rhathymum*$^{+}$	D	X	X	198	*Tripos muelleri*	R	X	X
148	*Prorocentrum rostratum**	D	X	X	199	*Tripos praelongus**	R		X

Continuation

ID	Species	OT	NC	SC	ID	Species	OT	NC	SC
	Dinoflagellates (cont.)					**Cyanobacteria**			
200	*Tripos setaceus**+	D	X	X	209	*Merismopedia tranquila**+	O	X	
201	*Tripos trichoceros**+	R	X	X	210	*Trichodesmium erythraeum*+	O	X	X
	Silicoflagellates					**Haptophytes**			
202	*Dictyocha calida**	D	X	X	211	*Phaeocystis pouchetii**+	O	X	X
203	*Dictyocha californica*+	D	X	X		**Euglenophytes**			
204	*Dictyocha fibula*+	D	X	X	212	*Eutreptiella marina*+	C	X	X
205	*Dictyocha fibula* var. *robusta*+	O	X	X		**Chlorophytes**			
206	*Dictyocha pentagona**	O	X	X	213	*Cosmarium* sp.*	R		X
207	*Octactis octonaria*+	D	X	X		**Ciliates**			
	Ebriids				214	*Mesodinium rubrum*+	D	X	X
208	*Hermesinum adriaticum**	R	X	X					

ness of 15-20 m that favors mixing and a thermocline defined at 20 m at station EN5. In SC, a high stratification of the water column is observed (1,093.82 J m^{-3}), with the thermocline defined at 50 m. Also observed in ES5 is the upwelling of cooler water (17.73°C) (Fig. 2). The NC presented lower values of salinity and density than the SC. This difference can probably be due to the influence of the Ameca River waters, which tend to deviate towards the NC due to the Coriolis effect, and this is related to the filament of <33.9 of salinity observed along the section.

On the other hand, in the SC, the filament of low salinity (<33.9) is also presented; likewise, a stratification effect of the water column by salinity and density appreciated (Fig. 2) due, probably, to the stabilization of the water column. Additionally, it can be observed that the entry of colder, saline, and denser water at the bottom of the ES5 station led to another upwelling event three days after our collection (February 24). The stabilization of the water column is due to the wind relaxation presented on the day of collection after the upwelling event that occurred on February 18 (NOAA 2024). Possible evidence of this event is the rise of the 21°C isotherm, which in SC is located at a depth of 30 m. At the same time, in NC, it was identified at 22 m, suggesting a water mass displacement gradient of ~0.3 m in the vertical for every kilometer in the horizontal direction. However, other factors to consider are the swells that occur during this period of the year due to their direct or indirect effect on the variations in the behavior of the water column, as well as the processes related to the internal waves that enter the NW part of the bay (Plata & Filonov 2007).

On both coasts, the pH in the bay did not show differences in the horizontal and vertical distribution, with an average record of 8.22 ± 0.15, with a difference of 0.5 between the range for both coasts (Fig. 2). Concerning dissolved oxygen and saturation, the highest values were found at the surface related to the exchange with the atmosphere by NW winds. In contrast, the lowest values were found at the bottom at stations EN5 and ES2 (Fig. 2). Values close to hypoxic conditions were recorded at a 20 m depth, according to the limit values determined by Vaquer-Sunyer & Duarte (2008) of 2 mg L^{-1}. Therefore, the low oxygen values obtained in our study may be related to both photosynthetic activity and organic matter degradation processes, given that at the surface, we found higher abundances of phytoplanktonic organisms compared to the bottom. The vertical and horizontal spatial distribution of the physicochemical variables presented in this study show a pattern similar to that reported by Bravo-Sierra (1999), Cepeda-Morales et al. (2009), Kelly-Gutiérrez et al. (2010) for the dry season in the study area.

Nutrients in the bay such as NH_4^+ recorded in NC and SC shows a homogeneous behavior in both vertical and horizontal distribution, with average concentrations of 4.03 µM (Fig. 3), where the highest value in this study (4.95 µM) is related to the algal bloom of the different dinoflagellates in EN2 at NC, and in ES1 (4.84 µM) is related to the abundance of diatoms at SC. In the case of NO_2^-, NO_3^-, and PO_4^{-3}, low values close to or equal to zero were recorded at the surface, and an increase in their concentration was observed as depth increased (Fig. 3). These lower values may be related to the consumption of these nutrients at the surface by phytoplankton, and the increase may be due to the action of vertical advection of water of subsurface origin associated with the upwelling recorded days before. The SiO_2 on both coasts presented a heterogeneous distribution both horizontally and vertically (Fig. 3). These low concentrations on the surface

Table 5. Summary of mean, standard deviation (SD), interval, and station recordings of groups of phytoplankton (cells L^{-1}) for sampling stations along the coast of Bahía de Banderas, Jalisco-Nayarit, Mexico in February 2022.

Phytoplankton groups	Mean ± SD	Station	Min	Max	Station	*H*	*P*
Diatoms	40,971 ± 65,279.22	EN5	500	295,880	ES1	16.11	0.07
Dinoflagellates	20,176 ± 19,879.38	ES2	1,740	80,260	ES5	5.54	0.79
Silicoflagellates	531 ± 224.08	ES2	160	1,000	ES3	14.61	0.10
Ebriids	11 ± 21.98	ES1	20	80	ES2	5.50	0.79
Cyanophytes	540 ± 1,339.44	EN3	400	5,000	ES2	7.16	0.62
Haptophytes	2,232 ± 6,679.32	ES2	100	25,880	ES5	11.84	0.22
Euglenophytes	19 ± 32.75	EN1, EN4, ES5	20	120	EN2	5.97	0.74
Chlorophytes	3 ± 9.79	ES4	20	40	ES5	8.45	0.49
Ciliates	2,197 ± 6,477.86	ES1, ES3	20	21,520	EN1	4.04	0.91

may be due to the assimilation of SiO_2 mainly by diatoms, which present high biomass in SC. The nutrient concentrations for the dry period in the bay are similar to those recorded by Kelly-Gutiérrez et al. (2010). Additionally, they noted that the Ameca River is one of the main contributors of NH_4^+, NO_2^-, NO_3^-, PO_4^{3-}, and SiO_2 compounds to the bay. We have also observed that the various rivers that flow into the bay in the SC contribute a large amount of nutrients, as do upwelling events, which contribute to making the PC abundant throughout the year.

On the other hand, López-Sandoval et al. (2009a) and Cortés-Lara et al. (2022) suggest that the conditions present during the dry season (winter-spring) in the BB, which are characterized by low temperatures, increased wind intensity, and water exchange due to upwelling processes increase nutrient availability, this, in turn, promotes phytoplankton growth and favors spring HAB events in the region; this, is related to the high Chl-*a* values recorded in this study (Fig. 4), where the values recorded for EN2 (28.11 mg m^{-3}) in NC and ES5 (21.30 mg m^{-3}) in SC associated with the biomass of the algal bloom that occurred in the BB due to the enrichment of the waters by the upwelling event, in which the ciliate *Mesodinium rubrum* and the dinoflagellates *Alexandrium tamiyavanichii* and *Prorocentrum lima* were the most abundant in EN2 and the diatoms *Leptocylindrus danicus*, *Guinardia striata* and *Chaetoceros curvisetus* in ES1, where in most of the bay the water coloration was golden-brown in SC and reddish in NC.

The different pigments (Chl-*b*, Chl-*c*, Chlo-Cya CARs, and Chr-Py CARs) presented the same behavior as Chl-*a*, where their maximum values are recorded in EN2 and ES5, being associated with the high biomasses of the different species mentioned above and the minimum values in EN5 and ES2 (Fig. 4). In addition, the aforementioned low oxygen levels are also evident at sites EN5 and ES2. These stations also recorded the lowest cell counts on both coasts, suggesting that, under hypoxic conditions, phytoplankton biomass and pigment concentrations are affected, with a tendency toward minimum values. In the case of phaeopigments, high values were observed at the bottom of both coasts (Fig. 4), although in the SC the average values 13.79 mg m^{-3}, which can be related to the depth of the water column in this area, because with the increase in the depth of the euphotic zone, the concentration of nutrients increases due to remineralization and accumulation of detritus (Lara-Lara & Álvarez-Borrego 1975) so, possibly these processes are responsible for the increase in the concentration of nutrients from 10 to 25 m in CN and at 25 m in SC.

The above is the result of complex and variable hydrographic, oceanographic, and anthropogenic environments in BB, both spatially and temporally. In this sense, studies conducted in the TPCM determine a well-defined seasonal pattern of high productivity along the coast in the cold period (winter-spring) associated with coastal upwelling and NW component winds (Espinoza-Carreón & Valdez-Holguín 2007, López-Sandoval et al. 2009a-b, Pérez-de Silva et al. 2023). Likewise, Cepeda-Morales et al. (2017) and Domínguez-Morales et al. (2020) define a 10 to 20 km wide strip of the coastal region, where primary productivity concentrated in chlorophyll is high (10-15 mg m^{-3}) throughout the year due to local processes and the intense dynamics of the region recording values greater than 20 mg m^{-3} at river mouths. Therefore, the results of this study are in line with the consensus that the highest chlorophyll concentration occurs during the last four months (February to May) of the dry period.

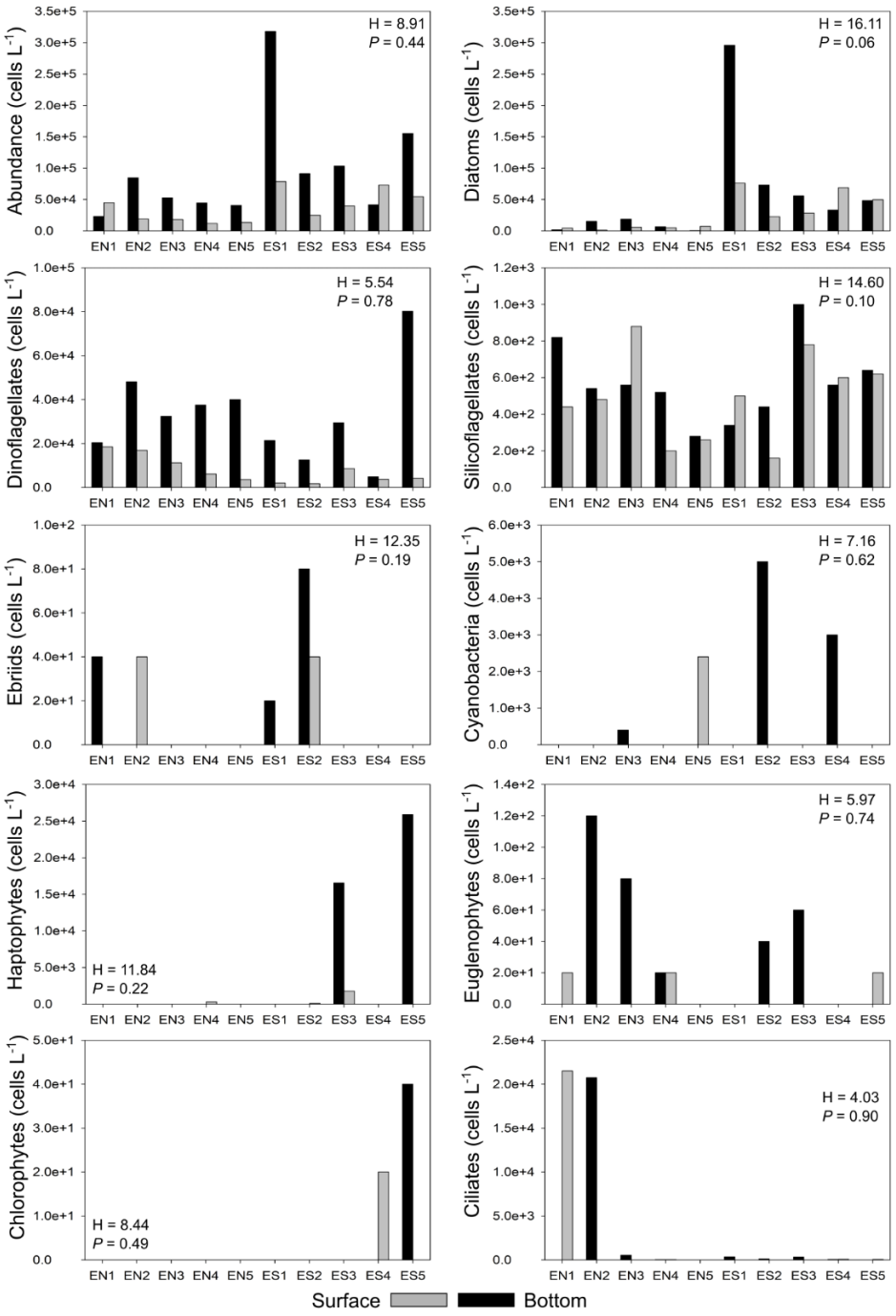

Figure 5. Cell abundances of the different groups that make up the phytoplankton community for each of the collection sites on the coasts of Bahía de Banderas, Jalisco-Nayarit, Mexico, in February 2022. Kruskal-Wallis test: H, *P*-value: *P*. Sampling stations; EN: north coast, ES: south coast.

Phytoplankton community (PC) and structure

The dominance of diatom and dinoflagellate groups characterizes the PC identified at BB, which is similar to what has been reported at different sites in the equatorial Pacific and the TPCM (e.g. Esqueda-Lara et al. 2005, Hernández-Becerril 2014, Estrada et al. 2016, Hernández-Becerril et al. 2021). In general, in BB, a greater presence of large-sized species and chain forms was observed, compared to small-sized species, which is consistent with that reported for the TPCM coasts (Chavez 1989). Likewise, richness and diversity were

Table 6. Summary of mean, standard deviation (SD), interval, and station recordings of diversity index of community of phytoplankton for sampling stations along the coast of Bahía de Banderas, Jalisco-Nayarit, Mexico in February 2022.

Diversity	Mean ± SD	Station	Min	Max	Station	*H*	*P*
Richness (S)	69.20 ± 14.03	EN5	45	99	ES1	14.08	0.12
Abundance (N) (cells L^{-1})	66,680 ± 69,179	EN4	11,780	317,980	ES1	8.91	0.45
Pielou's evenness (J')	0.61 ± 0.08	ES4	0.45	0.76	EN4	10.91	0.28
Shannon's diversity (H', bits)	3.70 ± 0.51	ES4	2.62	4.69	EN3	12.85	0.17
Simpson's dominance (λ)	0.17 ± 0.07	EN3	0.08	0.37	ES4	10.06	0.35
Simpson's co-dominance (1-λ)	0.83 ± 0.07	ES4	0.64	0.92	EN3	10.06	0.35

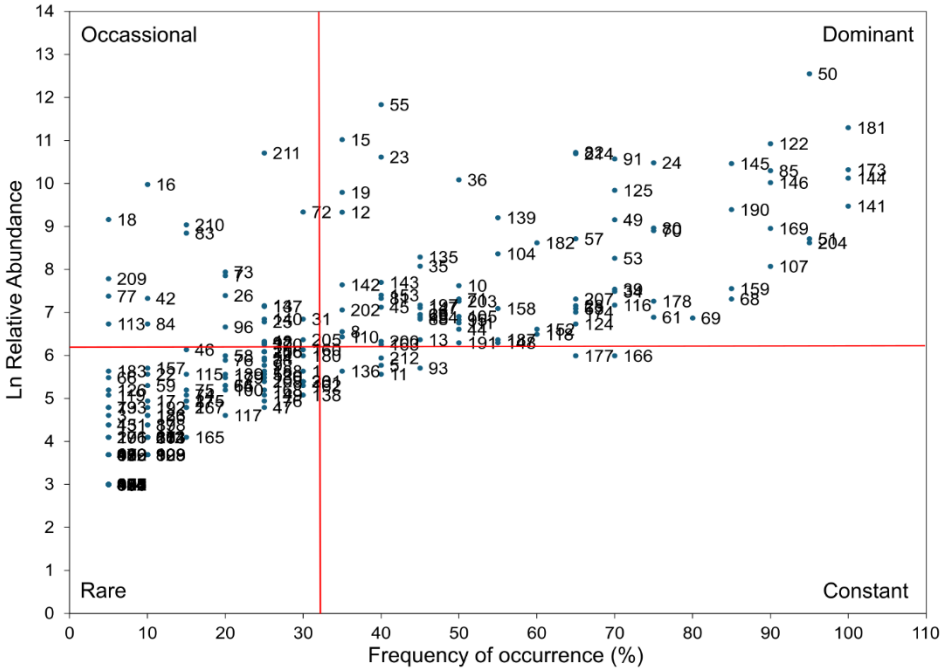

Figure 6. Olmstead-Tukey classification diagram for the phytoplankton community of Bahía de Banderas, Jalisco-Nayarit, Mexico in February 2022. The number corresponds to the species found in Table 4.

high on both coasts, with values of the Shannon-Weaver diversity index (H' >3.7) comparable to those determined for transition zones off (H' >3.0) and at the mouth (H' > 2.5) of the GC (Nienhius 1982, Gaxiola-Castro et al. 1987).

The results obtained in terms of richness (214 species) and abundance (<10^5 cells L^{-1}) are comparable with those reported by Bravo-Sierra (1999), who recorded up to 191 species during August and November 1990 and February 1991, classified into four groups. The results of the qualitative analysis of net samples in the study mentioned above showed that the lowest richness occurred in February (99 species), with diatoms (59) and dinoflagellates (38) as the dominant groups, and in smaller proportions, silicoflagellates (1) and cyanobacteria (1). Likewise, Cortés-Lara et al. (2022) reported the presence of 186 species during the period from 2000 to 2021, with a higher prevalence of diatoms (114) and dinoflagellates (61), and smaller proportion silicoflagellates (3), cyanobacteria (5), euglenophytes (1), ciliates (1) and raphidophyceae (1), highlighting abundances of the order of 10^6 cells L^{-1} for HAB species. In the present work, a higher number of species were identified than in the studies mentioned above, which may be due to the use of compound chambers employing the Utermöhl method (Reguera et al. 2011). This method is based on sedimentation of a 50 mL aliquot for species identification and quantification. In contrast, Bravo-Sierra (1999) used centrifugation and permanent slides for identification,

Table 7. Summary of the canonical correspondence analysis for environmental variables and species dominant of phytoplankton in sampling stations of Bahía de Banderas, Jalisco-Nayarit, Mexico in February 2022.

Axes	1	2	3	4	IT
Eigenvalues	0.195	0.038	0.024	0.021	0.571
Species-environment correlations	0.956	0.963	0.765	0.592	
Cumulative percentage variance					
Species data	34.2	40.8	45.0	48.6	
Species-environment data	61.9	73.9	81.5	88.0	
Sum of all eigenvalues					0.571
Sum of all canonical eigenvalues					0.315
Monte Carlo test			Eigenvalue	*F*	*P*
First canonical axis			0.195	5.194	0.0001
All canonical axes			0.315	1.371	0.1099

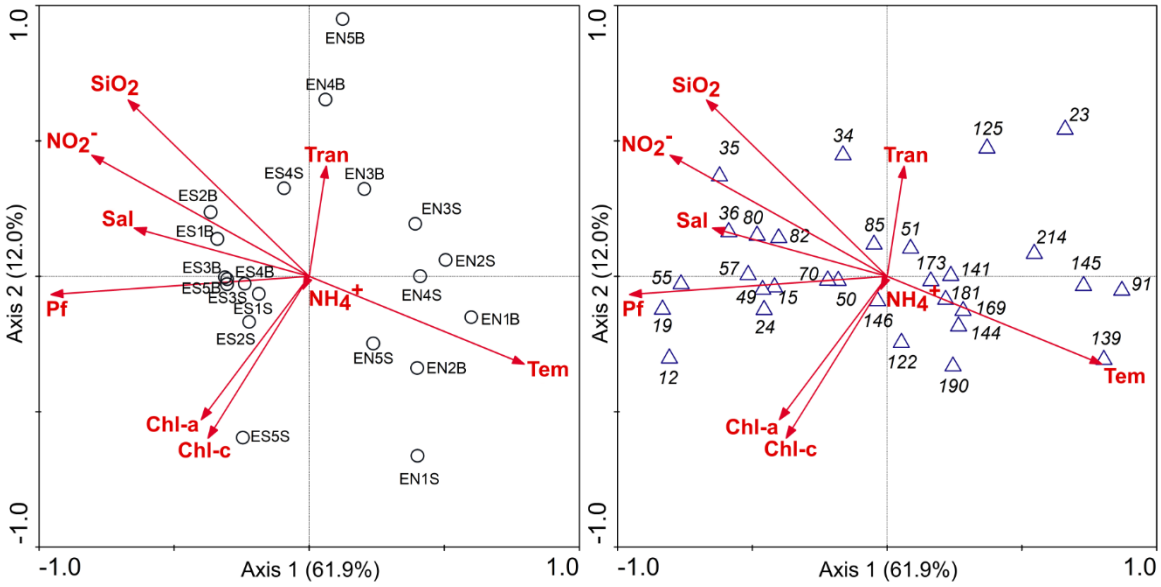

Figure 7. Canonical correspondence analysis between environmental variables and dominant species of the phytoplankton community in Bahía de Banderas, Jalisco-Nayarit, Mexico, in February 2022. Environmental variables and sampling stations for both coasts (left panel); and environmental variables and dominant species of the phytoplankton community (right panel), the number corresponds to the species found in Table 4. Sampling stations; EN: north coast, ES: south coast. S: surface; B: bottom.

while Cortés-Lara et al. (2022) employed a Sedgewick-Rafter chamber of 1 mL capacity, a more suitable method for estimating high cell densities, such as those present in the HAB events reported by the authors.

Six species were also identified as being present at all sampling stations (surface and bottom) on both coasts: the dinoflagellates *Prorocentrum gracile*, *P. micans*, and *Protoperidinium* spp., as well as the silicoflagellate *Dictyocha fibula*. These species are considered cosmopolitan. They are associated with temperate to warm temperatures and intermediate to high salinity waters. However, high-temperature and salinity conditions are considered ideal for their optimal growth (e.g. Hernández-Becerril & Bravo-Sierra 2001, Gribble et al. 2007, da Silva-Nunes et al. 2022). On the other hand, the low-temperature conditions in the water column in SC primarily favor the biomass of phytoplankton, mainly the diatoms group, which may be associated with the enrichment of the water by the upwelling event (February 18). Therefore, it is also possible that intensive grazing by zooplankton occurred. Furthermore, the group of ebriids, haptophytes, and chlorophytes are recorded for the first time in the bay and are integrated into the groups that can be found in the BB.

Phytoplankton and environmental variables relationship

The local atmospheric and oceanographic conditions that occur during the dry season in the bay showed that dinoflagellates presented a greater number of species (89) and cell abundances (234,740 cells L^{-1}) in NC, where a HAB was observed consisting of the species *Scrippsiella acuminata*, *Alexandrium tamiyavanichii*, *Margalefidinium polykrikoides* and *Prorocentrum gracile* and the ciliate *Mesodinium rubrum*. The dominance of dinoflagellates can be explained by the fact that on this coast, the platform is less deep and is more affected by the waves generated by the wind, which favors the resuspension of the cysts buried in the sediment and the subsequent mixing so that the water column maintains a higher temperature due to the gentle slope of the platform. On the contrary, in SC, there is a steeper slope and a greater depth of the water column, in addition to its orientation, which favors the presence of coastal upwelling due to NW wind action, which generates turbulence in the column and, therefore more favorable conditions for the growth of diatoms, which in this study showed a more abundance on this coast.

The CCA indicated that dinoflagellates presented a positive relationship towards environmental characteristics present in NC (Fig. 7), the environmental variables (Tem and Tran) associated with various dinoflagellate species, including, to mention, a few *Margalefidinium polykrikoides*, *Prorocentrum lima*, *P. gracile*, *Protoperidinium* spp., *P. pellucidum*, *Scrippsiella acuminata*, reveal a clear affinity to warm, low-transparency marine environments. This preference is linked to physiological adaptations that enable these to thrive under conditions where other phytoplankton groups, such as diatoms, are limited. These species exhibit optimal growth rates at temperatures above 24°C, which is common in tropical regions (Anderson 1998, Grzebyk et al. 2003). Additionally, their flagellated motility enables them to migrate vertically and position themselves in microenvironments with favorable light and nutrient conditions (Smayda 1997). Several of these species are also mixotrophic, a trait that provides a competitive advantage in turbid or stratified environments with limited light availability (Stoecker et al. 2017). Their proliferation is frequently associated with thermal stratification and eutrophication, particularly during warm periods or after continental discharge and upwelling events (Glibert et al. 2005). Many of these species, such as *Margalefidinium polykrikoides* and *Alexandrium tamiyavanichii*, are involved in HAB events, whose frequency has increased in coastal ecosystems affected by climate change and anthropogenic activities (Hallegraeff 2010, Griffith & Gobler 2020). Collectively, these ecological and physiological traits explain the dominance of these dinoflagellates in warm, low-transparency tropical coastal environments, such as those observed in NC.

On the other hand, in the SC (Fig. 7), diatoms (*Cerataulina pelagica*, *Chaetoceros* spp., *C. didymus*, *C. compressus*, *Leptocylindrus danicus*, *Lioloma pacificum*, *Guinardia flaccida*, *G. striata* and *Proboscia alata*) exhibit a strong association with the hydrographic conditions characteristic of this region, which include high concentrations of dissolved SiO_2, relatively low temperatures, intermediate to high marine salinities, and shallow or well-mixed water column. Dissolved SiO_2 is essential for their growth, as it constitutes the primary structural component of their frustules; thus, its availability largely regulates the biomass of this phytoplankton group (Brzezinski 1985, Dugdale & Wilkerson 1998). Although diatoms do not primarily utilize NO_2^- as a nitrogen source, they may indirectly benefit from their presence as an indicator of nutrient regeneration in areas where upwelling or remineralization processes occur, thereby promoting their proliferation (Dugdale et al. 1995, Clark et al. 2008). In terms of salinity, many species tolerate a wide range; however, marine species typically prefer salinities above 30, as observed in open coastal systems (Potapova 2011). Moreover, their distribution is strongly influenced by the physical dynamics of the water column. In shallow environments or under conditions of active vertical mixing, diatoms are retained in the euphotic zone; however, in stratified and deeper waters, they tend to sink rapidly (Kemp & Villareal 2013). Lastly, their abundance generally increases in cold or temperate waters, particularly in coastal upwelling regions where the combination of low temperatures and high nutrient availability creates optimal conditions for growth (Margalef 1978, Chavez & Barber 1987). Altogether, these factors explain the dominance of diatoms in highly productive oceanic zones such as continental shelves, eastern ocean margins, and estuarine systems influenced by upwelling and river discharge, as observed in the bay. Finally, having a positive correlation with pigments implies that the species were the main responsible for the high biomasses and high levels of Chl-*a* and Chl-*c* in the bay generated by the mixing of the water column due to the conditions generated by the NW winds and upwelling in the dry season in the BB region.

CONCLUSIONS

In the present study, the PC that we can find in the bay is enriched from 186 to 214 species, and it was found that dinoflagellates and diatoms were the dominant groups during the sampling conducted in February 2022, diatoms were positively correlated with the characteristics of the environmental variables of SC and dinoflagellates to those of NC. There are 83 new records for the bay, of which ebriids, haptophytes, and chlorophytes are groups that are recorded for the first time, increasing the total to 10 groups that can be found in the bay's water, increasing species richness and diversity.

The environmental variables presented similar characteristics to those presented in the TPCM; the thermocline, halocline, and pycnocline could be identified on both coasts. In NC, higher temperature, pH, dissolved oxygen, and saturation, as well as water column transparency, were recorded than in NC. In the SC, there was slight stratification of the water column, with a thermocline defined at 40 m. In addition, higher average values of salinity, density, nutrients, and pigments were recorded on this coast, which is related to the rise of subsurface water due to the upwelling event, thereby fertilizing the waters and increasing primary productivity in the euphotic zone.

The environmental variables considered satisfactorily explain the variability of phytoplankton composition. However, it is essential to continue systematic monitoring of phytoplankton and to incorporate additional physical, chemical, and biological variables to enhance the understanding of phytoplankton biomass dynamics in the BB, Jalisco-Nayarit, Mexico.

Credit author contribution

A.M. Cupul-Velázquez: conceptualization, fieldwork, methodology, formal analysis, investigation, writing and original draft; F. Vega-Villasante: conceptualization, supervisión, review & editing; M.C. Cortés-Lara: fieldwork, methodology and formal analysis; M.A. Fuentes-Arreazola: fieldwork, methodology and formal analysis; S.R. Guerrero-Galván: laboratory resources, review and editing; A.L. Cupul-Magaña: conceptualization, fieldwork, methodology, supervision, fundig acquisition, investigation, and review and editing. All authors have read and accepted the published version of the manuscript.

Conflict of interest

The authors declare no conflict of interest.

ACKNOWLEDGMENTS

This study was funded by project P0014-DCB-2020 by ALCM. The support 780865 by the Consejo Nacional de Humanidades, Ciencia y Tecnología de Mexico (CONAHCYT) for doctoral studies of AMCV is gratefully acknowledged.

REFERENCES

Anderson, D.M. 1998. Physiology and bloom dynamics of toxic *Alexandrium* species, with emphasis on life cycle transitions. In: Anderson, D.M., Cembella, A.D. & Hallegraeff, G.M. (Eds.). Physiological ecology of harmful algal blooms. Ecological Sciences, vol. 41. Springer, Berlin, pp 29-48.

Bravo-Sierra, E. 1999. Composición del fitoplancton de red en Bahía de Banderas, México, 1990-1991. Dissertation, Universidad Nacional Autónoma de México, Ciudad de México.

Brzezinski, M.A. 1985. The Si:C:N ratio of marine diatoms: interspecific variability and the effect of some environmental variables. Journal of Phycology, 21: 347-357. doi: 10.1111/j.0022-3646.1985.00347.x

Carriquiry, J.D., Cupul-Magaña, A.L., Rodríguez-Zaragoza, F., et al. 2001. Coral bleaching and mortality in the Mexican Pacific during the 1997-98 El Niño and prediction from a remote sensing approach. Bulletin of Marine Science, 69: 237-349.

Castro, R., Collins, C.A., Rago, T.A., et al. 2017. Currents, transport, and thermohaline variability at the entrance to the Gulf of California (19-21 April 2013). Ciencias Marinas, 43: 173-190. doi: 10.7773/cm.v43i3.2771

Cepeda-Morales, J., Beier, E., Gaxiola-Castro, G., et al. 2009. Effect of the oxygen minimum zone on the second chlorophyll maximum in the Eastern Tropical Pacific off Mexico. Ciencias Marinas, 35: 389-403. doi: 10.7773/cm.v35i4.1622

Cepeda-Morales, J., Hernández-Vásquez, F., Rivera-Caicedo, J., et al. 2017. Seasonal variability of satellite derived chlorophyll and sea surface temperature on the continental shelf of Nayarit, Mexico. Revista Bio Ciencias, 4: 17-34. doi: 10.15741/revbio.04.06.07

Chatterjee, S. & Hadi, A.S. 2012. Regression analysis by example. John Wiley and Sons, New York.

Chavez, F.P. 1989. Size distribution of phytoplankton in the central and eastern tropical Pacific. Global Biogeochemical Cycles, 3: 27-35. doi: 10.1029/GB003i001p00027

Chavez, F.P. & Barber, R.T. 1987. Na estimate of new production in the equatorial Pacific. Deep Sea Research - Part A: Oceanographic Research Papers, 34: 1229-1243. doi: 10.1016/0198-0149(87)90073-2

Clark, D.R., Rees, A.P. & Joint, I. 2008. Ammonium regeneration and nitrification rates in the oligotrophic Atlantic Ocean: Implications for new production estimates. Limnology and Oceanography, 53: 52-62. doi: 10.4319/lo.2008.53.1.0052

Cortés-Altamirano, R., Alonso-Rodríguez, R. & Peña-Ramírez, I. 1996-1997. Primer registro de marea roja debida a *Mesodinium rubrum* (Protozoa: Ciliata) en Bahía de Banderas, México. Revista de Biología Tropical, 44-45: 675-690.

Cortés-Lara, M.C., Cupul-Magaña, A.L. & Cupul-Velázquez, A.M. 2022. Fitoplancton marino de Bahía de Banderas con una revisión de los florecimientos algales nocivos en la región. In: Pérez-Morales, A., Galicia-Pérez, M.A. & Olivos-Ortiz, A. (Eds.). Estudios marinos y pesqueros en el Pacífico mexicano. Universidad de Colima, Colima, pp. 9-31.

Da Silva-Nunes, C.C., Lopes-da Silva, D.M., de Jesus-Affe, H.M., et al. 2022. Occurrence and distribution of *Scrippsiella* cf. *acuminata* (Dinophyta: Thoracosphaceae) in a tropical estuarine gradient. Rodriguésia, 73: e02162020. doi: 10.1590/2175-7860202273068

Domínguez-Hernández, G., Cepeda-Morales, J., Soto-Mardones, L., et al. 2020. Semiannual variations of chlorophyll concentration on the Eastern Tropical Pacific coast of Mexico. Advances in Space Research, 65: 2595-2607. doi: 10.1016/j.asr.2020.02.019

Dugdale, R.C. & Wilkerson, F.P. 1998. Silicate regulation of new production in the equatorial Pacific upwelling. Nature, 391: 270-273. doi: 10.1038/34630

Dugdale, R.C., Wilkerson, F.P. & Minas, H.J. 1995. The role of a silicate pump in driving new production. Deep Sea Research - Part I: Oceanographic Research Papers, 42: 697-719. doi: 10.1016/0967-0637(95)00 015-X

Espinoza-Carreón, T.L. & Valdez-Holguín, J.E. 2007. Gulf of California interannual chlorophyll variability. Ecología Aplicada, 6: 83-92. doi: 10.21704/rea.v6i1-2.344

Esqueda-Lara, K. & Hernández-Becerril, D.U. 2010. Dinoflagelados microplanctónicos marinos del Pacífico central de México (Isla Isabel, Nayarit y costas de Jalisco y Colima). Universidad Nacional Autónoma de México, Ciudad de México.

Esqueda-Lara, K., Hernández-Becerril, D.U. & Robles-Jarero, E.G. 2005. Annual cycle of microphytoplankton from the coasts of the tropical Mexican Pacific. Cahiers de Biologie Marine, 46: 335-345. doi: 10.21411/CBM.A.49037205

Estrada, M., Delgado, M., Blasco, D., et al. 2016. Phytoplankton across tropical and subtropical regions of the Atlantic, Indian, and Pacific Oceans. Plos One, 11: e0151699. doi: 10.1371/journal.pone.0151699

Fehling, J., Davidson, K., Bolch, C.J.S., et al. 2012. The relationship between phytoplankton distribution and water column characteristics in north west European shelf sea waters. Plos One, 7: e34098. doi: 10.1371/journal.pone.0034098

Fiedler, P.C. 1992. Seasonal climatologies and variability of eastern tropical Pacific surface waters. April 1992. NOAA Technical Report, NMFS: 109.

Field, C.B., Behrenfeld, M.J., Randerson, J.T., et al. 1998. Primary production of the biosphere: integrating terrestrial and oceanic components. Science, 281: 237-240. doi: 10.1126/science.281.5374.237

Gárate-Lizárraga, I. 2012. Proliferation of *Amphidinium carterae* (Gymnodiniales: Gymnodiniaceae) in Bahía de la Paz, Gulf of California. CICIMAR Oceánides, 27: 37-49. doi: 10.37543/oceanides.v27i2.115

Gárate-Lizárraga, I. 2014a. Proliferation of *Levanderina fissa* and *Polykrikos hartmannii* (Dinophyceae: Gymnodiniales) in Bahía de la Paz, Gulf of California, Mexico. CICIMAR Oceánides, 29: 25-35. doi: 10.37543/oceanides.v29i2.137

Gárate-Lizárraga, I. 2014b. Unarmored dinoflagellates present during a bloom of *Ceratoperidinium falcatum* in Bahía de la Paz, Gulf of California. Revista de Biología Marina y Oceanografía, 49: 577-587. doi: 10.4067/S0718-19572014000300014

Gárate-Lizárraga, I., Band-Schmidt, C.J., Aguirre-Bahena, F., et al. 2009. A multi-species microalgae bloom in Bahía de la Paz, Gulf of California, Mexico (June 2008). CICIMAR Oceánides, 24: 15-29. doi: 10.37543/oceanides.v24i1.50

Gaxiola-Castro, G., Nájera-de Muñoz, S. & Álvarez-Borrego, S. 1987. Winter phytoplankton of the Mexican Pacific Ocean. Ciencias Marinas, 13: 129-135. doi: 10.7773/cm.v13i4.549

General Bathymetric Charts of the Oceans (GEBCO). 2022. British Oceanographic Data Center. [https://www.gebco.net/data_and_products/gridded_bathymetry_data/gebco_2022/]. Reviewed: October 3, 2024

Glibert, P.M., Seitzinger, S., Heil, C.A., et al. 2005. The role of eutrophication in the global proliferation of harmful algal blooms, new perspectives and new approaches. Oceanography, 18: 198-209. doi: 10.5670/oceanog.2005.54

Gribble, K.E., Nolan, G. & Anderson, D.M. 2007. Biodiversity, biogeography, and potential trophic impact of *Protoperidinium* spp. (Dinophyceae) off the southwestern coast of Ireland. Journal of Plankton Research, 29: 931-947. doi: 10.1093/plankt/fbm070

Griffiths, R.C. 1968. Physical, chemical, and biological oceanography at the entrance to the Gulf of California, Spring of 1960. Special Scientific Report 573. US Fish & Wildlife Service. [https://spo.nmfs.noaa.gov/sites/default/files/legacy-pdfs/SSRF573.pdf]. Reviewed: November 6, 2024.

Griffith, A.W. & Gobler, C.J. 2020. Harmful algal blooms: a climate change co-stressor in marine and freshwater ecosystems. Harmful Algae, 91: 107590. doi: 10.1016/j.hal.2019.03.008

Grzebyk, D., Béchemin, C., Ward, C.J., et al. 2003. Effects of salinity and two coastal waters on the growth and toxin content of the dinoflagellate *Alexandrium minutum*. Journal of Plankton Research, 25: 1185-1199. doi: 10.1093/plankt/fbg088

Hallegraeff, G.M. 2010. Ocean climate change, phytoplankton community responses, and harmful algal blooms: a formidable predictive challenge. Journal of Phycology, 46: 220-235. doi: 10.111/j.1529-8817.2010.00815.x

Hays, G.C., Richardson, A.J. & Robinson, C. 2005. Climate change and marine plankton. Trends in Ecology and Evolution, 20: 337-344. doi: 10.1016/j.tree.2005.03.004

Hernández-Becerril, D.U. 2014. Biodiversidad de algas planctónicas marinas (Cyanobacteria, Prasinophyceae, Euglenophyta, Chrysophyceae, Dictyochophyceae, Eustigmatophyceae, Parmophyceae, Raphidophyceae, Bacillariophyta, Cryptophyta, Haptophyta, Dinoflagellata) en México. Revista Mexicana de Biodiversidad, 85: 44-53. doi: 10.7550/rmb.32037

Hernández-Becerril, D.U. & Bravo-Sierra, E. 2001. Planktonic Silicoflagellates (Dictyochophyceae) from the Mexican Pacific Ocean. Botanica Marina, 44: 417-423. doi: 10.1515/BOT.2001.050

Hernández-Becerril, D.U., Barón-Campis, S.A., Ceballos-Corona, J.G.A., et al. 2021. Catálogo de fitoplancton del Pacífico Central mexicano. Cruceros "MareaR" (2009-2019) B/O "El Puma". Universidad Nacional Autónoma de México, Ciudad de México.

Hernández-Becerril, D.U., García-Reséndiz, J., Salas-de León, D., et al. 2008. Nanoplankton fraction in the phytoplankton structure in the southern Gulf of Mexico (April 2000). Ciencias Marinas, 34: 77-90. doi: 10.7773/cm.v34i1.1263

Holm-Hansen, O. & Riemann, B. 1978. Chlorophyll-*a* determination: improvements in methodology. Oikos, 30: 438 447. doi: 10.2307/3543338

Ilyash, L.V., Radchenko, I.G., Shevchenko, V.P., et al. 2014. Contrasting summer phytoplankton communities in stratified and mixed waters of the white sea. Oceanology, 54: 730-738. doi: 10.1134/S0001437014050075

Instituto Nacional de Estadística y Geografía (INEGI). 2022a. Continuo de elevaciones mexicano. [https://www.inegi.org.mx/app/geo2/elevacionesmex/]. Reviewed: November 6, 2024.

Instituto Nacional de Estadística y Geografía (INEGI). 2022b. Geografía y ambiente, tema hidrología. [https://www.inegi.org.mx/temas/hidrologia/]. Reviewed: November 6, 2024.

Kelly-Gutiérrez, L.D., Plata-Rosas, L. & Guerrero-Galván, S. 2010. Bacteria prediction by means of Bayesian nets in Bahía de Banderas, Mexico. E-Gnosis, 8: 1-27.

Kemp, A.E.S. & Villareal, T.A. 2013. High diatom production and export in stratified waters-A potential negative feedback to global warming. Progress in Oceanography, 119: 4-23. doi: 10.1016/j.pocean.2013.06.004

Kirkwood, D.S. 1992. Stability of solutions of nutrient salts during storage. Marine Chemistry, 38: 151-164. doi: 10.1016/0304-4203(92)90032-6

Lara-Lara, J.R. & Álvarez-Borrego, S. 1975. Ciclo anual de clorofilas y producción orgánica primaria en Bahía San Quintín, B.C. Ciencias Marinas, 2: 77-97. doi: 10.7773/cm.v2i1.266

Lavín, M.F., Beier, E., Gómez-Valdés, J., et al. 2006. On the summer poleward coastal current off SW Mexico. Geophysical Research Letters, 33: L02601. doi: 10.1029/2005GL024686

Lavín, M.F., Castro, R., Beier, E., et al. 2009. SST, thermohaline structure, and circulation in the southern Gulf of California in June 2004 during the North America Monsoon Experiment. Journal of Geophysical Research, 114: C02025. doi: 10.1029/2008JC004896

Licea, S., Moreno, J.L., Santoyo, H., et al. 1995. Dinoflageladas del Golfo de California. Universidad Autónoma de Baja California Sur, Baja California Sur.

López-Sandoval, D., Lara-Lara, R., Álvarez-Borrego, S., et al. 2009a. Primary productivity in the eastern tropical Pacific off Cabo Corrientes, Mexico. Ciencias Marinas, 35: 169-182. doi: 10.7773/cm.v35i2.1530

López-Sandoval, D., Lara-Lara, J.R. & Álvarez-Borrego, S. 2009b. Phytoplankton production by remote sensing

in the region off Cabo Corrientes, Mexico. Hidrobiológica, 19: 185-192.

Margalef, R. 1978. Life forms of phytoplankton as survival alternatives in an unstable environment. Oceanology Acta, 1: 493-509.

Marshall, H.G. & Alden, R.W. 1993. A comparison of phytoplankton assemblages in the Chesapeake and Delaware estuaries (USA), with emphasis on diatoms. Hydrobiologia, 269: 251-261. doi: 10.1007/BF0002 8024

Matos, J.B., De Oliveira, S.M.O., Pereira, L.C.C., et al. 2016. Structure and temporal variation of the phytoplankton of a macrotidal beach from the Amazon coastal zone. Anais da Academia Brasileira de Ciências, 88: 1325-1339. doi: 10.1590/0001-3765201 620150688

Meave-del Castillo, M.E., Aké-Castillo, J.A., Zamudio-Reséndiz, M.E., et al. 2001. Registro de diatomeas planctónicas de las costas del Estado de Nayarit, México (Julio, 1999). Scientia Naturae, 3: 5-23.

Morales-Hernández, J.C., Farfán-Molina, L.M., Maciel-Carrillo-González, F., et al. 2013. Influence of the tropical cyclones between the period of 1970-2010 at the region of Banderas Bay, Nayarit-Jalisco, Mexico. Investigación y Ciencia, 59: 13-24. doi: 10.33064/ iycuaa 2013593705

Moreno, J.L., Licea, S. & Santoyo, H. 1996. Diatomeas del Golfo de California. Universidad Autónoma de Baja California Sur, Baja California Sur.

National Oceanic and Atmospheric Administration (NOAA). 2024. Upwelling index database. [https:// oceanview.pfeg.noaa.gov/products/upwelling/dnld]. Reviewed: November 3, 2024.

Nienhuis, H.J. 1982. Phytoplankton characteristics in the southern part of the Gulf of California. CIBCASIO Transactions, 6: 152-187.

Pantoja, D.A., Marinone, S.G., Parés-Sierra, A., et al. 2012. Numerical modeling of seasonal and mesoscale hydrography and circulation in the Mexican Central Pacific. Ciencias Marinas, 38: 363-379. doi: 10.7773/ cm.v38i2.2007

Pelayo-Martínez, G., Olivos-Ortiz, A., Franco-Gordo, C., et al. 2017. Physical, chemical, and zooplankton biomass variability (inshore-offshore) of Mexican Central Pacific during El Niño-La Niña 2010. Latin American Journal of Aquatic Research, 45: 67-78. doi: 10.3856/vol45-issue1-fulltext-7

Pérez-de Silva, C.V., Cupul-Magaña, A.L., Rodríguez-Zaragoza, F.A., et al. 2023. Temporal oceanographic variation using satellite imagery data in the central Mexican Pacific convergence zone. Ciencias Marinas, 49: e3260. doi: 10.7773/cm.y2023.3260

Plata, L. & Filonov, A. 2007. Internal tide in the northwestern part of Banderas Bay, Mexico. Ciencias Marinas, 33: 197-215. doi: 10.7773/cm.v33i2.1013

Portela, E., Beier, E., Barton, E.D., et al. 2016. Water masses and circulation in the Tropical Pacific off Central Mexico and surrounding areas. Journal of Physical Oceanography, 46: 3069-3081. doi: 10.1175/ JPO-D-16-0068.1

Potapova, M. 2011. Patterns of diatom distribution in relation to salinity. In: Seckbach, J. & Kociolek, P. (Eds.). The diatom world. Cellular origin, life in extreme habitats and astrobiology. Springer, Berlin, pp. 313-332.

Reguera, B., Alonso, R., Moreira, A., et al. 2011. Guía para el diseño y puesta en marcha de un plan de seguimiento de microalgas productoras de toxinas. UNESCO, Paris, pp. 59-65.

Round, F.E., Crawford, R.M. & Mann, D.G. 1990. The diatoms: biology and morphology of the genera. Cambridge University Press, Cambridge.

Schlitzer, R. 2024. Ocean Data View. [https://odv.awi.de]. Reviewed: November 3, 2024.

Simpson, J.H. 1981. The shelf-sea fronts: implications of their existence and behaviour. Philosophical Transactions of the Royal Society of London - Series A: Mathematical and Physical Sciences, 302: 531-546. doi: 10.1098/rsta.1981.0181

Smayda, T.J. 1997. Harmful algal blooms: their ecophysiology and general relevance to phytoplankton blooms in the sea. Limnology and Oceanography, 42: 1137-1153. doi: 10.4319/lo.1997.42.5_part_2.1137

Sokal, R. & Rohlf, F.J. 1981. Biometry: The principles and practice of statistics in biological research. Freeman, W.H., California.

Solórzano, L. 1969. Determination of ammonia in natural waters by phenol-hypochlorite method. Limnology and Oceanography, 14: 799-801. doi: 10.4319/lo.1969. 14.5.0799

Stoecker, D.K., Hansen, P.J., Caron, D.A., et al. 2017. Mixotrophy in the marine plankton. Annual Review of Marine Science, 9: 311-335. doi: 10.1146/annurev-marine-010816-060617

Strickland, J.H.D. & Parsons, T.R. 1972. A practical handbook of seawater analysis. Fisheries Research Board of Canada Bulletin, 157: 310.

ter Braak, C.J.F. 1986. Canonical correspondence analysis: a new eigenvector technique for multivariate

direct gradient analysis. Ecology, 67: 1167-1179. doi: 10.2307/1938672

ter Braak, C.J.F. & Šmilauer, P. 2002. CANOCO reference manual and CanoDraw for Windows user's guide: software for canonical community ordination (version 4.5). Microcomputer Power, Ithaca.

Troccoli-Ghinaglia, L., Herrera-Silveira, J.A. & Comín, F.A. 2004. Structural variations of phytoplankton in the coastal seas of Yucatan, Mexico. Hydrobiologia, 519: 85-102. doi: 10.1023/B: HYDR.0000026487. 78497.b6

Vaquer-Sunyer, R. & Duarte, C.M. 2008. Thresholds of hypoxia for marine biodiversity. Proceedings of the National Academy of Sciences, 105: 15452-15457. doi: 10.1073/pnas.0803833105

Received: December 5, 2024; Accepted: April 24, 2025

Wyrtki, K. 1965a. Surface currents of the eastern Pacific Ocean. Inter-American Tropical Tuna Commission Bulletin, 5: 271-304.

Wyrtki, K. 1965b. The annual and semiannual variation of the sea surface temperature in the North Pacific Ocean. Limnology and Oceanography, 10: 307-313. doi: 10.4319/lo.1965.10.3.0307

Zamudio, L., Hurlburt, H.E., Metzger, E.J., et al. 2007. Tropical wave-induced oceanic eddies at Cabo Corrientes and the Maria Islands, Mexico. Journal of Geophysical Research, 112: C05048. doi: 10.1029/ 2006JC004018

Zheng, Z., Hongjun, L., Wenli, S., et al. 2022. The large-scale spatial patterns of ecological networks between phytoplankton and zooplankton in coastal marine ecosystems. Science of the Total Environment, 827: 154285. doi: 10.1016/j.scitotenv.2022.154285